博士（工学）学位論文

Improving Generalization Ability of Estimation Models used in Sensing Technologies for Warehouse Management
（倉庫管理のためのセンシング技術における推定モデルの汎化能力向上方法に関する研究）

首都大学東京大学院システムデザイン研究科

Liang Shuyu

2019 年 8 月

指導教員　梶原　康博　教授

Contents

List of Figures

List of Tables

Abstracts

In distribution warehouses, work efficiency improvement is required to deal with increased shipping. In order to achieve work efficiency improvement, it is necessary to analyze workers' movements and ameliorate and automate their inefficient movements. What has been developed as warehouse management technologies for this purpose includes a sensing technology that uses image processing, radio waves and ultrasonic waves for the automation of movement analysis and a sensing technology that uses image processing for the automation of shipping volume inspection by the eye in order to shorten working hours and prevent shipping errors. However, the conventional methods while using sensing technologies have a defect since they do not take generalization ability of the estimation models into account. They provide good estimation performance from sensed past learning data, but they make large estimation errors in respect of unknown inspection data.

In this thesis, we propose a method aimed at improving the generalization ability of estimation models used in sensor systems for warehouse management. Based on optimization theory, system configuration and measurement/estimation models are designed according to functional requirements and environmental limitations. Considering realistic demand for warehouse management, sensor systems for indoor positioning, work analysis automation and counting automation are evaluated. This thesis is divided into five chapters:

Chapter 1 reviews the available research on the sensing technology used in logistics centers and describes common applications. The purpose and significance of the current studies are then presented, and the organization of the thesis is outlined.

Chapter 2 introduces the proposed method for measuring the position of workers or products inside a facility using RFID. The main problem with using RFID to track indoor positioning is caused by multipath, which significantly reduces the accuracy of

position estimation. Consequently, the proposed method seeks to reduce the adverse influence of multipath. In the proposed method, one or more tags can always be detected if multiple tags are attached to the target at different height. While varying the position of the positioning target, the reading rates for the tags can be obtained. A data set composed of the reading rates as input data and the positions of the positioning target as output data is then constructed. Using the generalization error as an index, an effective mathematical model for estimating the position of the positioning target from the input data is obtained. In an application example, the maximum value of the position estimation error for a stationary target was shown to be within 1.0m. Moreover, the height of the positioning target could be accurately estimated at all measuring points if the height difference between tags on the positioning target was at least 0.8 m. In a flow line investigation in which the target to be measured moved, the maximum value of the position estimation error was shown to be 0.5 m or less.

Chapter 3 describes the development of a work analysis support system for distribution processing and presents a case study featuring a retail clothing order fulfillment center. In this system, multiple ultrasonic sensors are used to measure a worker's flow line, and a smartphone is used to measure the worker's dominant hand acceleration. Models for estimating the worker's motion were derived from the obtained data. Candidate estimation approaches included the linear discriminant model, decision tree analysis, neural network and the k-nearest neighbor algorithm. The generalization error using cross-validation served as an index for choosing the optimal model. The support system obtains the described apparatus and methods for automating work analysis. The system was applied to an order-picking example at a clothing distribution center. The result of consistency test between the results obtained by video analysis and by support system was represented by kappa coefficient (κ). The value of κ was higher than 0.6, indicating that the work analysis result using the proposed system was acceptable.

Chapter 4 describes two methods and an apparatus for automatically counting the

number of stacked plywood sheets. The first method is a comparative method using image processing. Based on the normalized cross-correlation (NCC) method, this method can be used to detect plywood sheets, piece by piece. The second method is the proposed method. This method is based on the cross-validation method and uses an estimation model to determine the central portion of each plywood sheet in the cross-section. While using the proposed method, three candidate estimation approaches were evaluated: a statistically determined linear discriminant function, a decision tree, and a neural network, and the generalization error by cross-validation served as an index for choosing the optimal estimation model. In the application example of measuring about 450 to 500 common stacked plywood sheets with a standard thickness of 2.4 mm, both methods were able to correctly counting the number of plywood sheets. However, compared to the comparative method, the proposed method based on estimation model could significantly reduce the time required for counting.

Chapter 5 summarizes the findings of the study and proposes areas for further research. The expectation of improving generalization performance in actual logistics centers using the proposed method is discussed.

Chapter 1 Introduction

1.1 Research Background

Along with the application of information and communication technologies, there are new challenges generated for warehouse and distribution center management, such as: high speed for transparency, integrity control, and transformational agility [1, 2]. The logistics is becoming the centerpiece of a new business strategy featuring time-based competition and core competence along with the development of "smart factory logistics" [3]. Responding to these challenges, one of the most widely used technologies in the management system is the sensing technology. Using a wireless sensor network, it is possible to improve the work efficiency at work sites such as factory warehouses, distribution centers, and warehouse-style retail stores [4-6]. It is not a long time for the adoption of machine learning techniques used for estimation based on data obtained by wireless sensor networks, and still there are many problem needed to be resolved. For warehouse management, since nowadays the arrangements of inventory is in the midst of changes and the environment differs a lot for different sites, it is important to improve the generalization ability of estimation model using machine learning algorithms for unknown data.

1.1.1 Development of warehouse management

Warehousing has always being one of the most important subjects for companies, which is traditionally defined as the segment of an enterprise's logistics function responsible for the storage and handling of inventories beginning with supplier receipt and ending at the point of consumption, and the management of warehousing process is defined as warehouse management, including the maintenance of accurate and timely information relating to inventory status, location, condition, and disbursement [7].

The history of warehousing can be derived from the Age of Agriculture, however, the way how warehousing is performed has been changed along with the shifts of

customer behaviors. Gradually, products or materials needed for long-term storage are decreasing, and cross docking is becoming popular, especially where "just-in-time" is emphasized in traditional warehouse [8]. In order to improve customer serviceability, many technology equipped distribution centers are newly founded for products to be redistributed to retailers, to wholesalers, or directly to consumers. In these newly developed warehouses and distribution centers, products are constantly moved from being received, picked out according to dynamin orders and shipped out for delivery using warehouse management systems.

Under the sphere of competitive strategy for customers, "smart logistics" is now becoming a key competition force for many companies along with the development of industry and information technology [9]. A warehouse is no longer just a money and labor cost center, but a strategic place where automation, planning and execution technologies are needed for dynamic order fulfillment. Warehousing is changing to a core value added process, which provides time and place utility for transferring products through efficient management of space and time, and has various functions such as stockpiling, product mixing, and distribution [10]. Correspondingly, in the new generation, warehouse management is facing the challenge of providing manufacturers and distributors with unique avenues for competitive advantage, where digital work is needed for running up against the realities of the physical world such as storage, order picking, packing and checking items. Accordingly, various new technologies have been introduced to warehouse management system, and sensing technology is one of the most important technologies.

1.1.2 Sensing technologies used for warehouse management improvement

A sensor is a device that converts a physical phenomenon into an electrical signal. As such, sensors represent the interface between the physical world and the world of electrical devices, such as computers [11]. Sensing technology is applied by using various sensors. Sensors have been used in logistics for the last few decades and are of many types including light, temperature, motion and velocity sensors, etc. Numerous sensors now made warehousing functions once inconceivable reality.

However, these sensors cannot operate themselves, and they are only part of the wireless sensor networks (WSN), which is composed of a large number of sensor nodes that are densely deployed either inside the phenomenon or very close to it. [12]. WSN is usually applied to obtain required data through, and then the data will be used for processing by the other equipment in order to realize warehouse management improvement. That is to say, a system combining sensors and its assorted signal processing hardware with the processing either in or on the same package or discrete from the sensor itself is needed for the purpose of improvement. And here, the system is called a sensor system. In the sensor system, data is collected at the wireless sensor node, compressed, and transmitted to the gateway directly or, if required, uses other wireless sensor nodes to forward data to the gateway. The transmitted data is then presented to the system by the gateway connection [13].

There are three most prevailing WSN application scenarios including multiple-target tracking, surveillance, and vital sign and environmental critical monitoring [14]. For warehouse management, except relatively mature senor systems used for environmental critical monitoring, the sensor systems used for multiple-target tracking have been widely studied. There are many transmission options such as radio frequency identification (RFID) [15], bluetooth, ultrasonic wave [16], ultra-wideband(UWB) and several methods such as image processing, machine learning are used for indoor flow line measurement [17], which can be used to track real-time location of products or workers or robots used as workers. For example, smart distribution centers equipped with location tracking sensors are able to determine the precise positions of work-in-progress, tools and other production-relevant items within the facility.

The rapid development of high-functionality sensors brings a huge volume of sensing data gathered toward applications seeking to improve work efficiency. Multi-data confusion has been studied to combining data obtained by different sensors to resolve more complex problem. For example, automated guided vehicle systems (AGVSs) based on contact-free sensors are developed for automatic transportation in

warehouses [18]. Sensor and RFID (Radio Frequency Identification) networks have been also used for effective interaction and collaboration of decentralized E-Systems used for management improvement [19]. Besides, sensor systems have also been adopted for work automation in warehouse such as digital assorting system (DAS) and digital picking system (DPS) [20].

While designing sensor systems for measurement, it is very important to select an optimum sensors and wireless communications link to obtain accurate, reliable data since usually there are many options when selecting sensors, related equipment and communication platforms. Moreover, selection of the estimation model used in the system is also important, since whether or not the data churned out by the sensor system is used appropriately is the key influence factor for the general performance of the system. In another words, different estimation model with different characteristics will probably be subjected to different environments and different data requirements. The environment and requirements may also change even in the same warehouse. Correspondingly, the generalization ability of estimation model used in sensing technologies should also be monitored and improved in time to accommodate these changes.

1.1.3 Machine learning algorithms used in wireless sensor systems

In the late 1950's, Machine learning (ML) was introduced as a technique for artificial intelligence (AI) [21]. It has been used extensively for various tasks including classification, regression and density estimation in a variety of application areas such as computer vision, speech recognition, medical diagnosis, and marketing strategy. Over time, its focus evolved and shifted more to algorithms which are computationally viable and robust, and the algorithms and techniques used come from many diverse fields including statistics, mathematics, neuroscience, and computer science.

There is still no unified definition of machine learning. Generally, it is believed to be a process involving development of computer models for learning processes that

provide solutions to the problem of knowledge acquisition and enhance the performance of developed systems [22]. Machine learning is usually used to create prediction models using a collection of tools ad algorithms, and the algorithms can be divided by categories of supervised learning, unsupervised learning and reinforcement learning. While using machine learning for WSN, the historical data can be exploited to improve the performance of sensor networks on given tasks without the need for re-programming [23]. And machine learning is more suitable, when WSN are deployed in complicated environments where researchers cannot build accurate mathematical models to describe the system behavior, and when amounts of data obtained by WSN is required to be used to extract important correlations in them. Besides, machine learning is important to support decision-making and autonomous control for AI tasks with limited human intervention.

Unsupervised learning algorithms are mainly used for performing AI tasks, and reinforcement learning is suitable for WSN where each node seeks to choose actions that are expected to maximize its long term rewards. Supervised learning algorithms have been used for WSN in many aspects. The classic supervised learning algorithms and their characteristics and what type of problem they were suitable for are listed in Table 1-1 and Table 1-2, and they are usable for selecting machine learning algorithms used for estimation in sensor systems. In the present study, especially the ability of estimation model used in sensor systems is emphasized because of its different estimation performance while using constructed WSN for different tasks.

Table 1-1 Classic supervised learning algorithms and their applications

Supervised Learning Algorithm	Applicable Problem	Principle
Logistic Regression	· Binary Classification	Predicting the probability of occurrence of an event by fitting data to a logic function
Decision Tree	· Regression · Classification	The population is classified into two or more homogeneous sets based on most significant splitter/differentiator in input variables.
Neural Network	· Regression · Classification	The artificial neurons are interconnected and communicate with each other, and each connection is weighted by previous learning events and with each new input of data more learning takes place.
Linear Discriminant Function	· Linear Classification	Developing discriminant functions that are nothing but the linear combination of input variables that will discriminate between the categories of the dependent variables in a perfect manner.
Support Vector Machines	· Classification	Each data item is plotted as a point in n-dimensional space (where n is number of features you have) with the value of each feature being the value of a particular coordinate.
Naive Bayes	· Regression · Classification	A simple probabilistic classifier based on applying Bayes' theorem with strong (naïve) independence assumptions.
K-nearest Neighbor	· Regression · Classification	Storing all available cases and classifies new cases by a majority vote of its K neighbors.

Table 1-2 Advantages and disadvantages of classic supervised learning algorithms

Supervised Learning Algorithm	**Advantages**	**Disadvantages**
Logistic Regression	· Low variance · Provide probabilities for outcomes · Low computation cost · Easy to explain	· Prone to under-fitting · Not fit for multiple features · High bias
Decision Tree	· Less data cleaning required · Suitable for multiple data type · Non parametric method	· Prone to over fitting · Unsuitable for continuous variables · Possible issues with diagonal decision boundaries
Neural Network	· Suitable for large amount of data sets · Possible to implicitly detect complex nonlinear relationships between input and output variables · Ability to detect all possible interactions between predictor variables	· "black box" nature · Greater computational burden · Proneness to over fitting · Multi-layer neural network s are hard to train
Linear Discriminant Function	· Simple · Fast and portable · Good to use when beginning a project	· Require normal distribution · Not good for few categories variables · Suffer multicollinearity
Support Vector Machines	· Effective in high dimensional problem · Performs well with non-linear boundary depending on the kernel used	· Do not directly provide probability estimates. · Susceptible to over fitting/training issues depending on kernel
Naive Bayes	· Computationally fast · Simple to implement · Works well with high dimensions · Require less training data	· Relies on independence assumption and will perform badly if this assumption is not met
K-nearest Neighbor	· Simple and effective · Robust to noisy data by averaging k-nearest neighbors	· Computationally expensive · Distance between neighbors could be dominated by irrelevant attributes

1.2 Selection of three typical sensor systems used for warehouse management improvement

1.2.1 Influence factors for warehouse management cost

Averagely, warehouse management costs about 15%～25% of average in-stock value. It is an important management problem to reduce the warehouse management cost [24]. The constitution of warehouse management cost is described in Figure 1-1, and the key factors are mainly divided into three subjects including worker, inventory and facility and equipment. While working, a worker may do operations like replacing storage place for different items, finding out right items, picking out items, and confirming constitution and number of one bunch according to shipment order. Especially when the worker cannot pick out the right items needed for the next process in time, the production process will be affected and production cost will be increased. For in-stock inventory, the costs are related with the factors such as losing items, mis-shipment and other factors such as disposal, repack, repair and discounted goods. There are also costs related with facility and equipment used for warehouse management, such as idle space, construction cost, maintenance cost, utility cost, insurance and security cost.

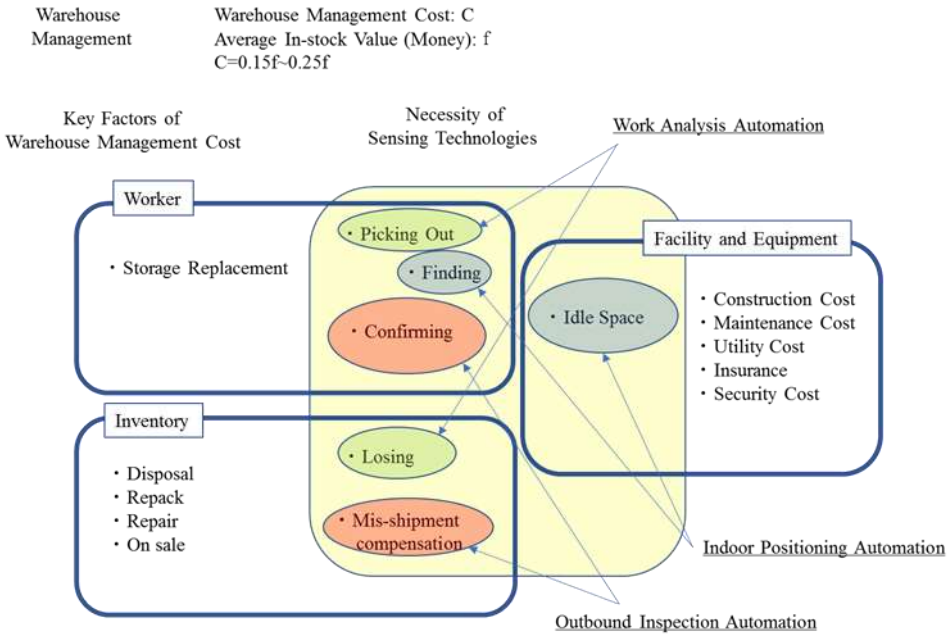

Figure 1-1 Constitution of warehouse management cost

1.2.2 Typical sensor systems used for reducing warehouse management cost

In order to reduce warehouse management cost, there are multiple methods can be used to improve related factors shown in Figure 1-1.However, sensing technologies are believed to be effective to reduce the cost caused by six factors of warehouse management, including finding items, picking out items, confirming order picking, losing items, mis-shipment, and idle space. Moreover, using sensing technologies, the information required for reducing warehouse management cost can be obtained automatically. So, it is possible to realize cost reduction more efficiently than the conventional manual method. That is also the reason why this thesis focuses on sensing technologies.

According to the necessary information needed for reducing cost, the six cost-related factors circled in Figure 1-1 can be divided into three categories which can be processed by different methods. The first method is defined as work analysis automation, which can be used to reduce the time needed for picking out items (work time) and to avoid losing items (Difference between actual inventory and recorded inventory). The second method is defined as flow line measurement automation, which is proposed to measure flow lines of both workers and in-stock items to reduce the time required for finding items and reduce the area of idle space. The last method is defined as outbound inspection automation, which is developed to reduce the time cost for outbound confirmation by at least two workers and avoid mis-shipment occasions. As shown in Figure 1-2, three typical sensor systems used for indoor object positioning, work analysis automation and visual inspection respectively are studied in the present study.

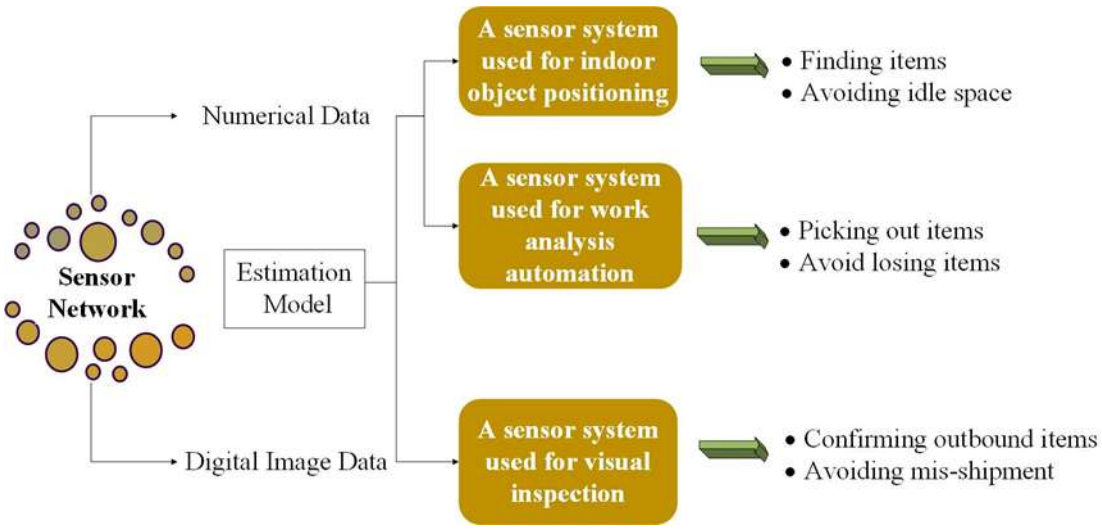

Figure 1-2 Typical three sensor systems proposed in the present study

1.2.3 Key Problems to be resolved for the selected sensor systems

It is crucial to analyze the key problems for selecting appropriate sensing technologies used in the three sensor systems.

Indoor positioning has been studied extensively for inventory management. However, because of the interference caused by obstacles such as pillars and shelves inside of the warehouses, the estimation accuracy is not high enough to find accurate position of an item while using sensor systems with respect to RFID, ultrasonic, or ZigBee. Therefore, the key problem to be resolved is to find a proper WSN and a method to reduce these influence caused by obstacles.

Traditionally, a worker's motion is usually recorded by a video camera, and then flow line measurement and work analysis will be realized by analyzing motions of the worker from the video. However, since there are many obstacles inside of the warehouses, the traditional method is difficult to be used to measure flow line, and it is also difficult for a worker's work analysis automation. Therefore, for work analysis automation, the key problem to be resolve is also caused by interference of pillars and shelves inside of warehouse. And except for image processing, there is still no other method designed for work analysis measurement automation.

Besides, while checking outbound items, taking an example of confirming the number of outbound items, at least two workers are engaged to accomplish the

inspection work, and the process is usually realized through manual visual inspection by the two workers. Although image processing has been widely used at production sites to automate visual inspection, it is difficult to be used in warehouse management because of the variety of shapes and colors of inventory items in outbound operations. So in this research, machine learning algorithms are proposed for automating outbound inspection. Since outbound items are very different from each other, the inspection system should be designed to different occasions. In this thesis, a method of automatically counting stacked plywood is proposed as a sample for outbound inspection.

1.3 Related Researches and Applications about the Proposed Three Typical Sensor Systems

1.3.1 Researches on indoor positioning of stationary objects

Accurately acquiring the positions of people and objects existed in multiple places in production systems is essential for warehouse management automation, and is very helpful to ensure the workers' safety, especially in logistics centers. When estimating positions of multiple indoor objects, the methods including image processing, ultrasonic or radio wave are usually used [25-27]. Using the method of image processing, it is hard to accurately estimate the positions since the perspective is usually interrupted by obstacles such as mechanical equipment at the production sits [28]. Using the method of ultrasonic, it is difficult for long time positioning since the driving time of the battery used as ultrasonic power source is limited [29].

Global Positioning System (GPS) using radio wave signals is not appropriate for indoor positioning since these signals are also easily sheltered by obstacles [30]. Indoor Messaging System (IMES) using radio waves has been used for the indoor positioning [31]. In this system, several transmitters were installed to the ceiling and a receiver is attached to the positioning target, while measuring, the position of the target is estimated to be the position of the transmitter from which the received signal is strongest, and the estimation accuracy is estimated to be one to ten meters [32].

There are also some methods proposed for position estimation using wireless LAN equipment [33]. In a method, a radio wave transmitter was attached to an object, and several receivers were installed to surroundings. The transmitter's position was estimated by angel of arrival (Angle of Arrival, AOA) and received signal strength (Received Signal Strength, RSS) of radio waves received by the receivers. Since the value of RSS decreases when the transmitter moved away from the measured receiver, the distance between the transmitter and the receiver was estimated based on RSS. When there are multiple receivers, the transmitter's position can be calculated by geometry method using the position and the value of AOA and RSS got by the transmitter from each receiver. When using this method, there is also a problem of multipath propagation caused by reflection surfaces indoors, and hence the estimation error is great. In another method, the position was estimated using location fingerprint which is represented by different characteristics of received signals (AOA, RSS, etc.) got from multiple Access Points (APs), and the transmitter's position is estimated through matching the observed location fingerprint with the fingerprint database [34].

Instead of wireless LAN equipment, Radio Frequency Identifier (RFID) recently has been used widely for position estimation [35], since the RFID tags used in which are cheaper than a radio wave transmitter such as smartphones, and these tags are also easier to be attached not only to workers and parts, but also materials (circulation box, component palette) needed to be carried outside of the plants. Additionally, each of the attached RFID tags has a certain identification number (ID), so it is possible to estimate the position using multiple tags. The main parameter used in RFID method is reading rate, which must be sufficiently high to ensure an object state changes can be continuously and faultlessly captured [36]. Sadr et al. proposed a model to estimate a tag's position using a quadratic probability density function representing the relationship between the tag's position and the reading rate [37]. In another proposal, similarly using the relationship, Sekiguchi et al. established a position estimation model using the neural network to distinguish a tag's position [38]. But there is still a problem while using the two methods: the maxima of estimation errors are both

higher than 1.5 m. One of the main reasons is also believed to be radio interference caused by multipath reflected by surroundings.

In conclusion, RFID has been widely used for indoor positioning mainly because of its easy deployment and low cost [39], and it is also appropriate for positioning in warehouse or logistic centers [40]. However, in order to improve generalization performance of RFID systems, the problem of radio interference is needed to be resolved to reduce the estimation error, especially in warehouse and distribution centers since there are so many obstacles such as shelves, pillars, and other equipment.

1.3.2 Researches on automation of distribution processing analysis

Distribution processing is generally defined as a series of work steps, including picking, sorting, inspecting, and packing items to fulfill online retail orders [41]. The efficiency of the work is one of the most important subjects in logistics. Additionally, the cost of order picking is estimated to account for more than 55% of the total labor cost at logistic centers [42]. To date, many studies have evaluated picking efficiency. Enkawa et al. focused on the moving time for picking work, and theoretically derived an evaluation scale for choosing between single picking and total picking based on the IQ curve, which represents the number of goods issued for each item [43]. Another study concluded that the working time needed for order picking varies according to the operator's skill [44]. Therefore, to promote the efficiency of distribution processing, practical work analysis is important to redesign the influencing factors in the system, such as stock allocation and work allocation.

Video analysis is widely used as a means of work analysis [45], but it has a problem in that too much time is spent analyzing the videos and determining the flow line of each operation in detail. Thus, research in automating work analysis has been conducted. However, so far automation has been studied separately for the measurement of working time, motions in three-dimensional space and flow line.

Regarding motions, the working time for different motions, such as moving,

loading, or unloading, can be measured by changes in the worker's posture, which can be detected by a motion capture device [46]. This method has an estimation accuracy higher than 95% when compared to the results of video analysis, which has been experimentally confirmed. However, it is inconvenient for a worker to wear acceleration sensors all over the body at all times while working, which is necessary for the motion capture device. Additionally, this method is difficult to use for flow line measurement because estimation error of the waist position may accumulate as time goes by. Another method using Kinect was also proposed to measure motion [47]. This method has the merit of measuring the flow line and motion simultaneously, but it is not applicable when the measurement range is wide or the environment is exposed to direct sunlight.

In order to analyze working time, a system using a range image sensor has been developed [48]. However, its measurement range, about 5m both in length and width, is too narrow and the measurement conditions require no obstacles, such as shelves and pillars. In another related research, a method for analyzing the work time of workers was developed based on using a video camera [49]. In this method, a worker's position is detected using the histogram of gradient (HOG) from video records, and then by classifying the changes in HOG feature quantities using a support vector machine (SM), one of the optimization methods, the worker's motion and time used for each motion are analyzed. Comparing the method using range image, this method has the advantage of wider measurement range.

For position measurement in three-dimensional space, a method utilizing stereo vision was developed to measure movement by tracking multiple markers attached to pedestrians [50]. The process of getting a marker's three-dimensional coordinate is as follows: The coordinate of the marker is detected in two-dimensional images captured by multiple cameras, and then its three-dimensional position is obtained using the direct linear transformation (DLT) method, which is based on the least squares method. In the studies mentioned above, optical equipment was used. However, it is not suitable for logistics centers since there are many obstacles, such as shelves and

pillars that hinder the vision field of the optical equipment. Therefore, it is hard for work analysis when using optical equipment, such as cameras or range image sensors.

Automation of flow line measurement has been realized using acceleration sensors [51]. The flow line is obtained using the moving distance, which is calculated by integrating the corresponding accelerations twice. For this kind of method, the measurement accuracy is reported to be 0.45 m(standard deviation$\pm$0.23 m) along the x axis and 0.27 m(standard deviation $\pm$ 0.21 m) along the y axis when the measurement area is about16 m $\times$ 30 m. It is believed that the measurement error is accumulated every time the direction of the acceleration sensor changes while moving. In logistics centers, the worker's moving direction changes so frequently that it may lead to a result where the estimation error is too large. Radio frequency identification (RFID) has been used to measure flow lines [52]. The tag reading rate (= number of successful readings/number of attempted readings) decreases inversely according to the increase in distances between the radio transmitter and tags. It was reported that the average error for estimating the tag position is 0.3 m and the maximum error is 0.7 m. Moreover, the RFID devices are expensive if the measurement range must cover the entire indoor area of a large facility. Compared to the RFID method, image processing is much cheaper when used to measure the flow line [53]. Still, it has the problem of being easily affected by changes in the indoor lighting environment due to the weather or time of day. There is also a method used to detect the operator based on properties such as clothing colors, but detection becomes difficult when the flow lines of many operators cross over each other.

Finally, a method using ultrasonic sensors was developed for flow line measurement [54]. Although the arrival distance of the ultrasonic wave is shorter than that of the radio waves used in the RFID method, its transmission speed is much lower, so it can be used to measure the flow line more accurately. The equipment is also much cheaper. Since both the flow line and worker’s motion are required to be measured for analyzing distribution process, an ultrasonic system is believed to be more appropriate in real time over a wide area.

1.3.3 Researches on visual inspection

Ultrasonic test equipment is generally used to check for adhesion failure in plywood sheets [55]. Image processing devices have already been developed for surface quality inspection; for example, to check the wood grain, and for pinholes and other surface defects [56]. However, the number of plywood sheets in a stack is still checked by visual inspection in most situations, and an automated method for performing this task is urgently needed.

Image processing is widely used for the automation of visual inspection. When a certain kind of object is known and the objects are laid flat on a workbench, the number of objects can be measured using a labeling method [57]. In the situation in which the shape of the object is coin-like, the quantity of the objects can be measured using Hough transformation, even if there are some overlaps [58]. Moreover, if there is a pattern on the object, template matching can be used for inspection. Template matching methods can be roughly divided into two types: (1) methods that use a feature value extractor for gathering and organizing information concerning objects in an image, and (2) object detection methods based on feature values. Many basic statistic variables, such as the mean brightness, unbiased variances, such as the mean brightness, unbiased variance, and standard deviation, can be used as feature values [59]. However, these values are easily affected by changes in lighting conditions, such as external light intensity.

Therefore, it is necessary to find a method that is sufficiently robust against changes in lighting conditions. A number of methods have been proposed. One method applies a two-dimensional Fourier transformation to an image and then uses the power spectrum obtained as the feature value [60]. Another method is the eigenvalue method [61], which has been shown to be effective for reducing the number of reference images and strengthening robustness against changes in lighting conditions. The method used for object detection should allow the highest degree of similarity for the detection of the image moves. Since there is no consensus on the definition of the degree of similarity, there are a number of methods that use different

measures for the degree of similarity. For example, the normalized cross-correlation (NCC) method uses normalized cross-correlation, the sum of squared differences (SSD) method uses the sum of squared differences, and the sum of absolute values of differences (SAD) method uses the sum of absolute values of the differences [62]. Since the NCC method is used to normalize brightness, it is more robust against changes in lighting conditions than the SSD method or SAD method. However, its computational complexity is much higher than that both the SSD method and SAD method.

Since all three methods need to compare the brightness of all pixels in the inspection image, a large amount of calculation is required. Accordingly, a new method should be developed in order to reduce the calculation load for template matching. Among the various existing methods, object detection by means of estimation model is of particular interest. In methods using this technique, an image can be represented by a small number of feature values, and object detection can be performed based on these values using an estimation model such as a linear discriminant function, neural network, or decision tree. The control variables of the estimation model are set such that the residual sum of squares is minimized using learning data. For example, the linear discriminant function has been used to inspect the appearance of disposable wooden chopsticks [63]. The neural network has been used for defect inspection, such as inspections for bent or misaligned connector plug pins [64]. By providing an intermediate layer for the neural network and virtually creating a high-dimensional pattern space, it is possible to detect defects that could not be successfully identified using the linear discriminant function. The decision tree method has been used to recognize road signs using a car-mounted camera [65]. Compared to the linear discriminant function and neural network, the decision tree has the advantage of lower calculation cost. The estimation performance of these estimation models is investigated based on the generalization error, which is widely used in statistical learning theory [66].

In addition to image-processing methods, a method for estimating the number of

sheets of a material by measuring the height of the stacked sheets with laser sensor and dividing the height of the stack by the thickness of one sheet has also been proposed [67]. This method is based on the premise that the material of the sheet is sufficiently hard (e.g., steel) and the machining accuracy for the sheet thickness is assumed to be sufficiently high. According to JIS standard G3141, the tolerance for 2.4 mm thick steel sheet is ± 0.12 mm. However, according to the Japanese Agricultural Standard, the tolerance for a 2.4 mm thick plywood sheet is ± 0.2 mm, which is significantly higher. Furthermore, since there are also allowable values for warpage and torsion of the plywood sheet, gaps between plywood sheets can occur during loading. Therefore, it is difficult to accurately measure the number of stacked plywood sheets by measuring the stack height.

Based on the above considerations, the present study focuses on the development of methods that can quickly and accurately measure the number of plywood sheets in a stack based on conventional image-processing methods.

1.4 Research Objectives and Significations

1.4.1 Purpose of the study

No matter in a traditional warehouse or a distribution center, technology development is emphasized for warehouse management to realize “smarter”

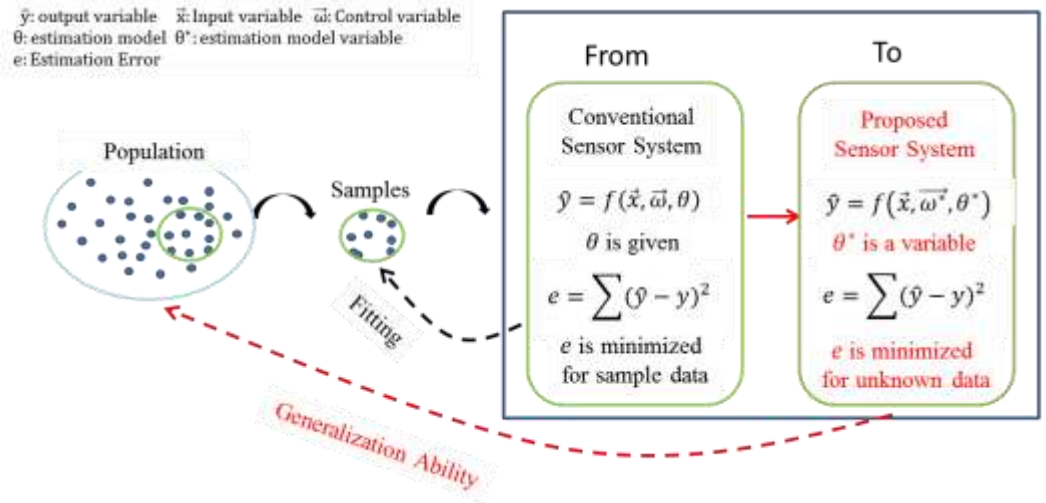

Figure 1-3 Optimization of estimation model used in sensor systems for warehouse management

management and control. As known, various sensing technologies have been introduced to these technology-enhanced warehouses and logistics centers.

Traditionally, sensor systems are usually used to minimize the measurement or estimation error over past sample data. However, composition of objects is changing in shorter and shorter cycles in logistics centers, and real-time visibility and workforce interaction is needed for improving work efficiency inside of warehouses. In order to make sure those sensor systems could be operated stably and efficiently, it is necessary to improve the generalization ability of estimation model based on unknown data in real-time. Generally, the purpose of the study is to propose a general optimization method of proposing several candidate algorithms used for estimation method in sensor systems used for warehouse management improvement, which is shown in Figure 1-3.

For the section of indoor positioning, the purpose is to propose a method of suppressing the influence of radio interference for indoor positioning by RFID to enhance the accuracy of position estimation, which could be used for finding out mistake in loading and unloading pallets, automating judgement of the shelft height, and judging whether a worker is standing or lying on the floor to make sure his safty.

For the section of improving picking efficiency, the main purpose is to develop an inexpensive support system for work analysis and then import it to the work site for use in measuring the flow line and working time of the different motions in real time over a wide area used for distribution processing. The system should be useful for redesigning the influence factor in the system, speeding up the development of handling products, shortening the time needed for work improvement and shifting the responsibility for these activities from industrial engineering experts to on-site supervisors or small groups formed by employees.

For the section of visual inspection, since the number of plywood sheets must also be checked during the shipping process, the main purpose is to develop a automate system for counting the number of stacked plywood sheets which is very different

with other sheets, and is hard to be realized through traditional sensor methods. The system should be simple and economical for the application in warehouse.

1.4.2 Significance of the study

This study provides a view of sensor system optimization used for warehouse management, which has not been studied before. Also, optimization method is used in three typical sensor systems for object positioning, work analysis automation and automatic counting of stacked plywood sheets.

Traditionally, the estimation method is defined mainly based on samples selected from unknown data, which is hard for evaluation of system performance. In our study, several algorithms are proposed based on samples, and then the performance of different algorithms is evaluated through application example to choose the best solution according to specific environments.

For estimation of indoor object position, a new method is proposed for suppressing the interference of reflected radio waves for indoor positioning based on RFID. The work analysis automation system used acceleration sensors to obtain data used for flow line measurement and motion identification, which is economical and easy to use. For visual inspection, machine learning is newly adopted to automatically counting stacked plywood sheets.

In conclusion, estimation models are determined by comparing the performance of different machine learning algorithms using the data obtained by sensors, and machine learning used for estimation in these sensor systems provides an example for development of intelligent factory.

1.5 Thesis statement

This study focuses on how to improve the generalization ability of estimation models used in sensor systems for warehouse management, and the thesis is divided into five chapters:

Chapter 1 reviews the available research on the sensing technology used in

logistics centers and describes common applications. The purpose and significance of the current study are then presented, and the organization of the thesis is outlined.

Chapter 2 introduces the proposed method for measuring the position of workers or products inside a facility using RFID. The main problem with using RFID to track indoor positioning is caused by multipath, which significantly reduces the accuracy of position estimation. Consequently, the proposed method seeks to reduce the adverse influence of multipath. In the proposed method, one or more tags can always be detected if multiple tags are attached to the target at different height. While varying the position of the positioning target, the reading rates for the tags can be obtained. A data set composed of the reading rates as input data and the positions of the positioning target as output data is then constructed. Using the generalization error as an index, an effective mathematical model for estimating the position of the positioning target from the input data is obtained. In an application example, the average value of the position estimation error for a stationary target was shown to be 0.02 m. Moreover, the height of the positioning target could be accurately estimated at all measuring points if the height difference between tags on the positioning target was at least 0.8 m. In a flow line investigation in which the target to be measured moved, the average value of the position estimation error was shown to be 0.29 m.

Chapter 3 describes the development of a work analysis support system for distribution processing and presents a case study featuring a retail clothing order fulfillment center. In this system, multiple ultrasonic sensors are used to measure a worker's flow line, and a smartphone is used to measure the worker's dominant hand acceleration. Models for estimating the worker's motion were derived from the obtained data. Candidate estimation approaches included the linear discriminant model, decision tree analysis, and the k-nearest neighbor algorithm. The generalization error using cross-validation served as an index for choosing the optimal model. The support system obtains the described apparatus and methods for automating work analysis. The system was applied to an order-picking example at a clothing distribution center. The result of consistency test between the results obtained

by video analysis and by support system was represented by kappa coefficient (κ). The value of κ was higher than 0.6, indicating that the work analysis result using the proposed system was acceptable.

Chapter 4 describes two methods and an apparatus for automatically counting the number of stacked plywood sheets. The first method is a comparative method using image processing. Based on the normalized cross-correlation (NCC) method, this method can be used to detect plywood sheets, piece by piece. The second method is the proposed method. This method is based on the cross-validation method and uses an estimation model to determine the central portion of each plywood sheet in the cross-section. While using the proposed method, three candidate estimation approaches were evaluated: a statistically determined linear discriminant function, a decision tree, and a neural network, and the generalization error by cross-validation served as an index for choosing the optimal estimation model. In the application example of measuring about 450 to 500 common stacked plywood sheets with a standard thickness of 2.4 mm, both methods were able to correctly counting the number of plywood sheets. However, compared to the comparative method, the proposed method based on estimation model could significantly reduce the time required for counting.

Chapter 5 summarizes the findings of the study and proposes areas for further research. The expectation of improving estimation model generalization ability in actual logistics centers using the proposed method is discussed.

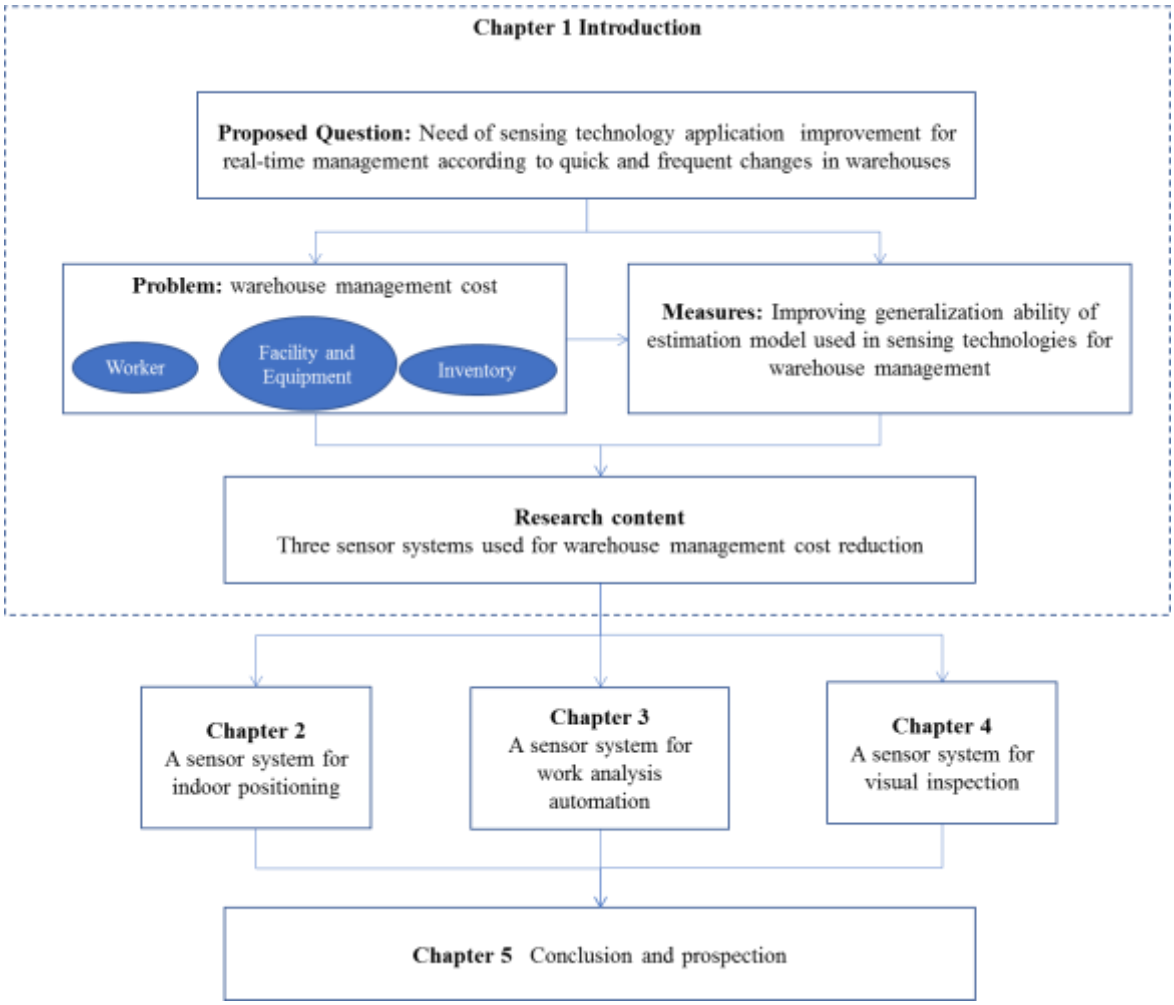

Figure 1-4 Organization of the study

Chapter 2 A sensor system for indoor object positioning

2.1 Introduction

In this chapter, an indoor positioning method using RFID is proposed to reduce influence of radio interference on positioning accuracy. The principle used here is that one or more tags can always be detected if multiple tags are attached at different heights to one target. The reading rate of a tag is expressed as a ratio of the number of read attempts of the tag to the number successful reads while varying the position of the positioning target. A data set comprising reading rates as input data and positions of the positioning target as output data is obtained for estimation. Then, using the generalization error as an index, a mathematical model for estimating the position of the positioning target from the input data is obtained using the data set. In an application example, the maximum value of the position estimation error of a stationary target is shown to be within 1.0 m, and the height of the positioning target could be accurately estimated at all measuring points if the height difference between tags on the positioning target is at least 0.8 m. Furthermore, in a flow line investigation, in which the target to be measured moves, the maximum value of the position estimation error is shown to be 0.5 m or less.

2.2 RFID system

2.2.1 The architecture of the system

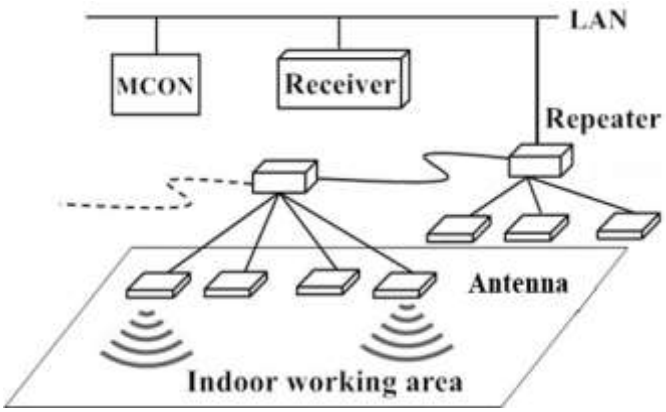

Figure 2-1 Architecture of RFID system

The RFID system used in this study is mainly constituted by several antennas, a receiver and a master controller (MCON), and its architecture is shown in Figure 2-1. The antennas are installed vertically downward the roof, which will send out radio signals once received instruction from the MCON, and meanwhile electric power will be supplied to tags sprinkled throughout the measurement area to activate these tags. Each of the activated tags will then transmit wireless message including information of its ID and the antenna ID which provide the electric to the receiver, and after that, positions of these tags will be estimated mainly according to value of reading rates calculated by the MCON.

2.2.2 Key factors related with the system

As mentioned before, reading rate is just the parameter used for location estimation in our system. Here, reading rate r is defined as a ratio of the number of read attempts of the tag q to the number successful reads q_0 for a receiver while varying position of the positioning target. The reading rate r can be calculated using Eq. (2.1).

$$r = {}^{q}/_{q_0} \qquad (2.1)$$

While a tag is moving, reading rate will be measured for each antenna. That is to say, once a tag is moved, reading rates of each installed antenna will be recorded for all the measurement positions of the tag which are indicated by coordinates. Theoretically, value of an antenna's reading rate is very close to 1 when a tag is located nearby the area directly under the antenna, and the value will become smaller and smaller as the tag moves away from the antenna, and finally the value will be 0 if the tag is out of the antenna's communication area. However, according to actual observations, sometimes value of the reading rate is also 0 while a tag is just located nearby the area directly under the antenna (hereafter referred to as Null Point). If there is no other system problem such as not strength enough electric field for motivating a tag, one very important reason for Null Point is believed to be radio interference caused by the wave reflected by the other objects, which means there are multi radio

waves from different paths received by the tag, and the next section will give a detailed explanation of the interference caused by multi paths.

There are different shape formats of antennas such as linear and planar, and distribution of each antenna's electric field intensity varies for different shapes. Here, in this study, non-directional antenna is used to analyze the influence of the reflected waves from the floor surface on the distribution of the electric field intensity. The propagation paths of a direct wave and a reflected wave transmitted from an antenna for a tag are shown in Figure 2-2.

Height of the antenna (Position A) is indicated as h_1, and height of the tag (Position B) is indicated as h_2. Horizontal distance from the antenna to the tag is denoted as α. Then length of the direct wave can be represented as ($l_1 = \sqrt{\alpha^2 + (h_1 - h_2)^2}$), and length of the reflected wave as ($l_2 = \sqrt{\alpha^2 + (h_1 + h_2)^2}$). If the wave length is λ, a phase lag ($\varphi = \delta + \psi$) will be generated between the direct wave and the reflected wave, which is consisted of the lag ($\delta = 2\pi(l_1 - l_2)/\lambda$) due to the path length difference and the lag ψ due to the reflection. Therefore, the phase lag φ is proportional to the path length difference $(l_1 - l_2)$. If electric field intensity at point A is denoted as E_0, at point B, electric field intensity of the direct wave E_1 and electric field strength of the reflected wave E_2 can be represented by the following equations, which are inversely proportional to the square of their path length.

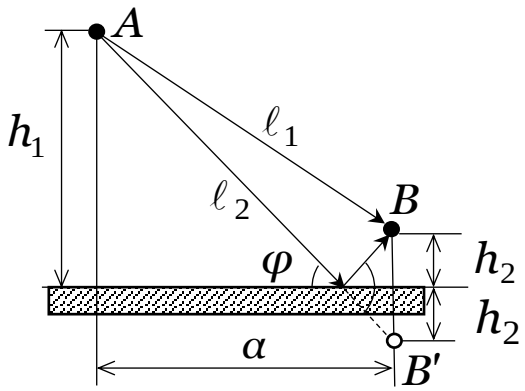

Figure 2-2 Propagation path of a direct wave and a reflected wave

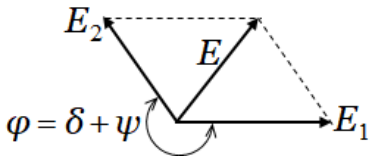

Figure 2-3 Combination wave of direct wave and reflected wave

$$E_1 = \frac{E_0}{4\pi l_1^2} \tag{2.2}$$

$$E_2 = \frac{E_0}{4\pi l_2^2} \tag{2.3}$$

Accordingly, electric field intensity E at point B is the combination of E_1 and E_2. Since there is a phase lag φ between the direct wave and the reflected wave, the relationship of E_1 and E_2 is shown in Figure 2-3. E is obtained by decomposing parallel and perpendicular components of E_2 and E_1, and it can be calculated through Eq. (2.4) based on Euclidean Distance.

$$\begin{aligned} E &= \sqrt{(E_1 - E_2 \cdot cos(\varphi - \pi))^2 + (E_2 \cdot sin(\varphi - \pi))^2} \\ &= \sqrt{E_1^2 + E_2^2 - 2E_1E_2\, cos(\varphi - \pi)} \end{aligned} \tag{2.4}$$

In Eq. (2.4), because E_1 and E_2 are inversely proportional to square of the path length and φ is proportional to $(l_1 - l_2)$, received electric field intensity E changes in accordance with path length changes. As a result of this, a null point is likely to occur in the region where the value of E is small.

2.3 Proposed Method

At a Null Point, it is difficult to estimate whether a tag is in the communication area or not only from an antenna's reading rate. Accordingly, a method of reducing influence of Null Point is proposed, which intends to estimate a tag's position by reading rates obtained from multiple antennas. The proposed method includes two parts: estimating position and height of a stationary object and estimating flow line of a moving object. The floor surface is defined as a XY coordinate system, and it is divided into fixed intervals both in X axis direction and Y axis direction. In this method, center of each segment is defined as a measurement point, and an object is

estimated which segment (measurement point) it is located in.

2.3.1 Measures to reduce the influence of multi radio wave paths

Inside a tag, an internal antenna will be electromotive once received a radio wave signal, and the generated alternating current electricity will then be converted to direct current to provide electric power needed for operation of a control circuit by a rectifier. As a result, it is believed that the higher electric field intensity a tag received, the easier the tag activated, which also means a higher reading rate. According to Eq. (2.4), even if horizontal distance from an antenna to tags with different height is identical, their radio wave path length will be different and electric field intensity for different tags will be different. Therefore, a method of using tags attached to different height of the object is proposed in the system.

Besides, position estimation accuracy for an object is believed to be higher when an antenna's reading rate decreases smoothly according to the increase of horizontal distance from the antenna to the object than the case where the reading rate changes irregularly. For purpose of regular changes, reading rate for an antenna is defined to be a compound value obtained from tags with different height, using reading rate of each tag multiplying by its weighting coefficient. Theoretically, reading rate of a tag is considered to be proportional to the electric field strength it received. So, the weighting coefficient will be obtained based on the electric field intensity got from Eq. (2.2) and Eq. (2.4). If coordinate of the center (the point directly under the antenna) is denoted as (x_o, y_o), coordinate of the measurement point away from the center by α distance is supposed to be (x_α, y_α).

$$\alpha = \sqrt{(x_\alpha - x_o)^2 + (y_\alpha - y_o)^2} \qquad (2.5)$$

When the horizontal distance α is changing across over the entire communication area, the electric field intensity at any measurement point could be represented as $f(\alpha)$ without considering the reflected waves by the floor. Similarly, for tags at different heights of this measurement point, the electric field intensity obtained by Equation

(2.4) at the height of jth tag is denoted as $f_j(\alpha)$. Then there will be a compound value combining reading rates for all the tags at the measurement point, which is the sum of $f_j(\alpha)$ multiplying by its coefficient w_j. The difference between the compound value and $f(\alpha)$ is expressed in the following equations.

$$E(\vec{w}) = \int_0^{\infty} \left| f(\alpha) - \sum_{j=1}^{J} w_j \cdot f_j(\alpha) \right|^2 d\alpha$$

$$\text{Except}, \sum_{j=1}^{J} w_j = 1, w_j \geq 0 \qquad (2.6)$$

The weighting coefficient $\vec{w}^*$ is determined by least square method to ensure that the result of Eq. (2.6) is minimized.

A numerical example is proposed to explain how to calculate the weighting factors considering the radio interference due to floor reflection. In this example, the height of the installed antenna is 2.9 m, and the wavelength of the transmitted radio wave is 0.33 m. It is assumed that the electric field strength around the antenna surface is $E_0 = 1$. Without considering the floor reflection, Figure 2-4 (a) shows distribution of electric field intensity for a tag installed at the height of 1.0m above the floor due to free propagations. The electric field intensity decreases smoothly as the tag moved away from the area directly below the antenna. For tags installed at height of 1.1m，1.0m，and 0.9m, distributions of the electric field intensity obtained by Eq. (2.4) is shown separately in Figure 2-4 (b)～(d) for each tag. According to these figures, the position where the electric field strength is small is different for each of the three tags. In order to minimize the value of Eq. (2.5), the weighting coefficients for the three tags should be adjusted according to the electric field strength shown in Figure 2-4, and numerically the coefficients is obtained by least square method: $w_1 = 0.28$, $w_2 = 0.46$, $w_3 = 0.26$. The distribution of the weighted electric field intensity is shown in Figure 2-4 (e), and the amplitude is obviously reduced compared to any other three results for each tag. Consequently, it is visible that the compound value obtained from the above procedure will also decrease smoothly as the horizontal distance from the antenna to the three tags increases.

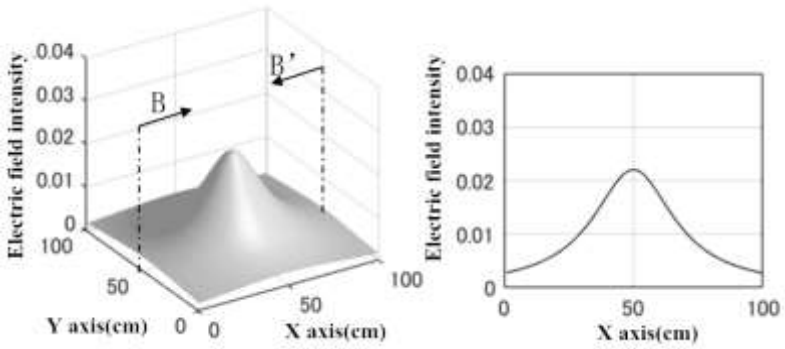

(a) Electric field strength due to free propagations and the strength of B-B'cross section

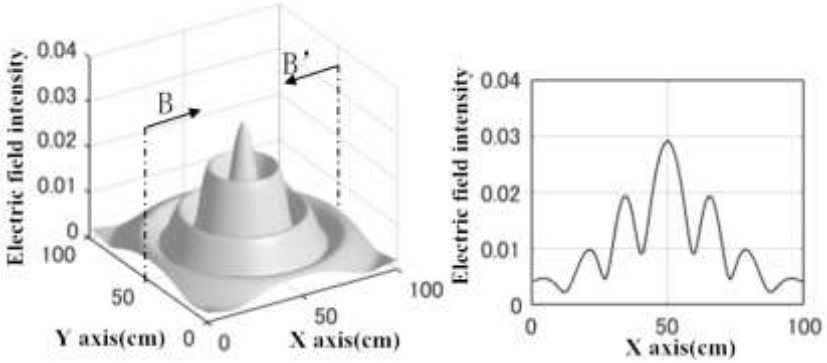

(b) Electric field strength at height of 1.1m and the strength of B-B'cross section

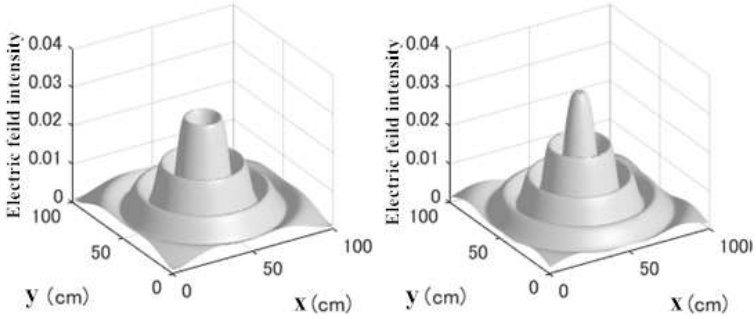

(c) Electric field strength at height of 1.0m (d) Electric field strength at height of 1.0m

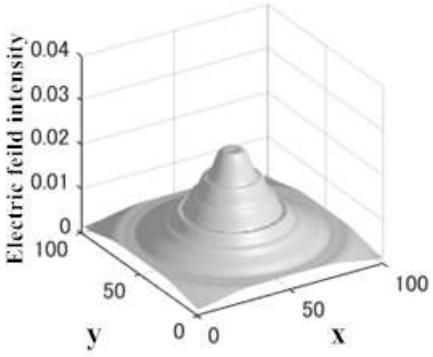

(e) Weighted electric field strength

Figure 2-4 Distribution of electric field intensity

However, besides the floor, the radio wave can also be reflected by other objects at production site such as wall, mechanical equipment, and workers, so the weighting coefficient should be reconsidered according to the shape of the antenna and the production environment. Therefore, $w_j = 1/J$ is usually defined as original value for all the weighting coefficients. In the following section, the weighting coefficients will be modified according to the environment after selecting the model for indoor positioning. In the continuation, the reading rate for each antenna is represented by a compound value obtained from reading rates of multiple tags multiplying by their weighting coefficients.

2.3.2 Selection of estimation model

Theoretically, the shorter the radio wave wavelength, the narrower the communication area of the antenna. In order to ensure an effective communication area and increase the number of variables used for estimating the position of a stationary object, radio waves with different radio frequencies should be sent out by each installed antenna. Radio frequency is usually measured by power, and this study, we call that radio wave output level. Reading rate of each antenna at every measurement point is measured. While measuring, an object attached with a plurality of tags is moved back and forth and right and left at regular intervals, and reading rate of each antenna is measured at every measurement point during the process. After that, an estimation model is determined to represent the relationship between a measurement point and corresponding reading rate of each antenna. It is assumed that the relationship is linear or nonlinear. If the relationship is linear, linear discriminant function can be considered as the estimation model, and if the relationship is nonlinear, decision tree method, k-nearest neighbor algorithm, and neural network (hereinafter, NN) can be considered as candidate models. Generalization error obtained by k-fold cross-validation method is used as an index for evaluating estimation performance of these models [68]. Number of installed antennas is denoted as n_1, and number of the radio wave output levels is denoted as n_2. Then, reading rate of an antenna at any measurement point can be denoted as a $N(= n_1 \times n_2 \times J)$

dimensional input vector, $\vec{r} = (r_1, \cdots, r_n)^T \in R^N$, and the measurement point is represented by an output value $y \in R$. The total number of the input/output pairs is defined as M, and the i th pair can be denoted by $(\vec{r_i}, y_i)$. If the control variable $\vec{\omega}$, and the estimation model variable θ are defined, then the estimation model for the input/output pair can be expressed as follows:

$$y = f(\vec{r}, \vec{\omega}, \theta) \tag{2.7}$$

For example, when the estimation model variable θ is decision tree model, elements of the control variable $\vec{\omega}$ are branching conditions of nodes in a classification tree. The collection of input/output pairs is represented by a data set $D = \{(\vec{r}_1, y_1), \cdots (\vec{r}_M, y_M)\}$. Data set D is divided equally into K groups, and the uth test set is $C_u, (u = 1, \cdots K)$. If the test set C_u is removed from the data set D, we can obtain the training data set $L_u (= D \backslash C_u)$. The training data set is used to obtain the control variable of the estimation model. The test set is used to estimate the output value and estimate the error from the input vector once the control variable is determined. The generalization error $A(\theta)$ obtained by K-fold cross-validation method is expressed as follows:

$$A(\theta) = \frac{1}{2} \sum_{u=1}^{K} \sum_{(\vec{r}, y) \in C_u} (y - f(\vec{r}, \vec{\omega}_u^*, \theta))^2 \tag{2.8}$$

The data set is divided into a training set and a test set for the calculation of $A(\theta)$. Using $f(\vec{r}, \vec{\omega}_u^*, \theta)$, which uses the best fitting control variable $\vec{\omega}_u^*$, for training set L_u, the performance of the estimation model can be asymptotically evaluated if we can accurately determine whether the test data are properly associated with the training data. Then, the model with the smallest generalization error $A(\theta)$ is selected as the estimation model. The estimation model is determined using the above procedures. Once the estimation model is determined, newly input data are analyzed to identify the motion in real time.

2.3.3 Rectification of weighting coefficients

In Section 2.3.1， the original weighting coefficients are all represented by $w_j =$

$1/J$, and reading rate at a measurement point is just the average value of reading rates for tags at different heights. However, in actual indoor positioning environment, there are many other reflection waves caused by objects such as wall, mechanical equaipments and workers, and therefore the position estimation error of estimation model θ may not be minimized using the average value of the reading rates. Then, after selecting the estimation model θ in Section 2.3.2, the weighting coefficients which could be represented by an invector $\vec{w} = (w_1, \cdots, w_J)$ will be modified to make sure that the position estimation error could be minimized with respect to the data set D. Position estimation error for dataset D is shown in Eq. (2.9). Under the constraint condition of Eq. (2.6), weighting coefficient w_j of each tag is changed in increments of 0.01 within a range of zero to one, and finially the invector $\vec{w}$ will be modified to satisfy Eq. (2.10).

$$\sum(\vec{w}|D) = \sum_{(\vec{r},y)\in D}\left(y - f(\vec{r}, \theta, \vec{w})\right)^2 \qquad (2.9)$$

$$\vec{w}^* = arg\ \min_{\vec{w}} \sum(\vec{w}|D) \qquad (2.10)$$

2.3.4 Flow line correction

When estimating an moving object's flow line, it is difficult to measure reading rate using different radio wave frequencies since the object only stay a very short time at a measurement point. Accordingly, in order to shorten measurement time for estimation of an object's flow line, a single radio wave output is used. If there is only one tag attached to the moving object, it is believed the position estimation error is too large because the existence of Null Point, and correspondingly Moving Average Method is used to correct flow line of the moving object. Estimated position $(x_i, y_i)$is obtained in chronological order, and if the number of measurement points used for Moving Average Method is denoted as m, the moving average value of the X coordinates can be calculated by Eq. (2.11), while the moving average value of the Y coordinates can be calculated by Eq. (2.12).

$$xx_i = \frac{\sum_{c=i-m+1}^{i} x_c}{m} \qquad (2.11)$$

$$yy_i = \frac{\sum_{c=i-m+1}^{i} y_c}{m} \qquad (2.12)$$

2.4 Application Example

2.4.1 Installation of an RFID system

In present study, an RFID system manufactured by Mojix was used, and main specifications of the system would be described as follows. Directivity of the receiver was 120 degrees in horizontal plane and 90 degrees in vertical plane, and the maximum communication distance between the receiver and a tag was about 200 m. As a consequence, the maximum value of communication area was about 25,000 m^2. The receiver could be connected with 2048 antennas in maximum, and each antenna could motivate the tags within a communication distance of 10 m. UHF band (920 MHz band) radio waves were selected for the experiment. There were 11 antennas installed vertically downward at the height of 2.9 m above the floor, and the distribution is shown in Figure 2-5. Measurement points were set at intervals of 0.5 m both in the X-axis direction and the Y-axis direction within the 5 m × 7 m measurement area, and so there were finally 117 measurement points in the measurement area.

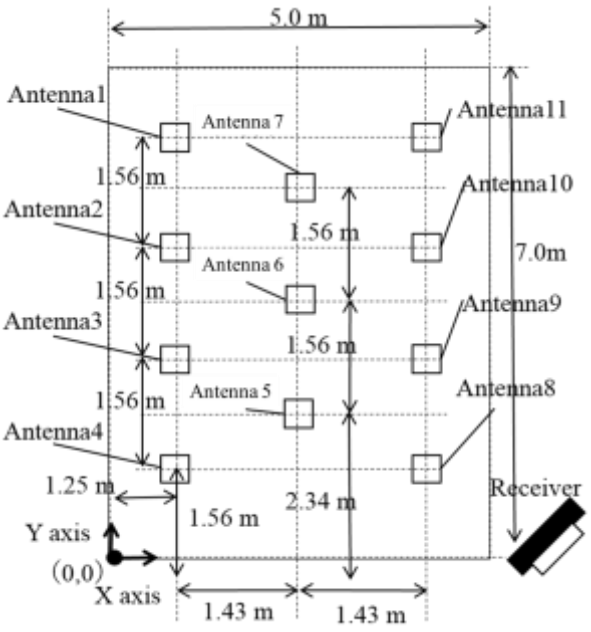

Figure 2-5 Allocation of all the antennas

2.4.2 Compare of reading rates got by one tag and three tags

The number of reading attempts by the control PC (MCON) was 60.5 times/sec on average, and the number of reading attempts for each antenna was 5.5 times/sec (= 60.5 / 11) when there were 11 antennas in the measurement area. The reading rate of antenna 6 in the center of the measurment area was firstly measured. Within its communication area, there was no mechanical equipment which could obstruct the radio wave conduction. The distance from antenna 6 to the wall was both 3 m in the X-axis direction and the Y-axis direction. A tag is attached to an object at the height of 1.0 m, and the object was moved back and forth and left and right at 0.5 m intervals. The tag stayed for ten seconds at every measurement point, and during this period the coordinates of the measurement point and the reading rate of antenna 6 were recorded after the reading rate became stable.The measured distribution of reading rate is shown in Figure 2-6. Generally, the reading rate decreased as the object moved away from the center (0,0) just directly under antenna 6. However, there were points(Null Points) where the reading rate was 0 in the vicinity of the area directly under the antenna.

In the following experiment, a worker was defined as the measurement object. Acordding to the height of the worker's feet, waist and head, three tags were attached to the worker at the height of 0.15 m, 1.0 m, and 1.5 m, and the worker was moved horizontally back and forth and right and left. The average reading rates of antenna 6 got by the three tags at every measurement point were shown in Figure 2-7. Compared with Figure 2-6, occurence of Null Point was suppressed. However, although generally the reading rate decreased as the worker moved away from the space just directly under the antenna, there were also irregularly changes during the process.

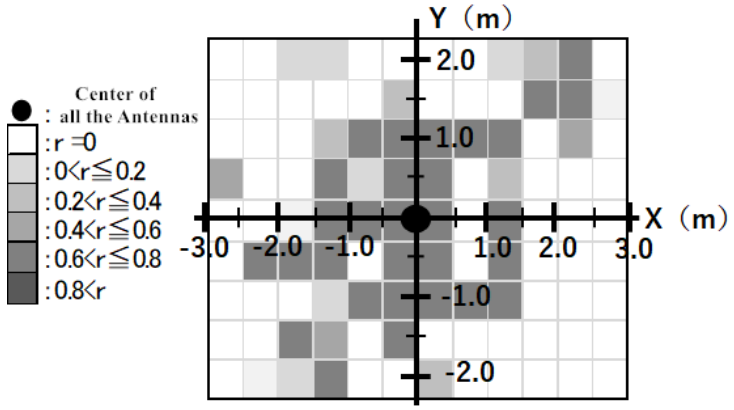

Figure 2-6　Reading rate of antenna 6 when using one tag

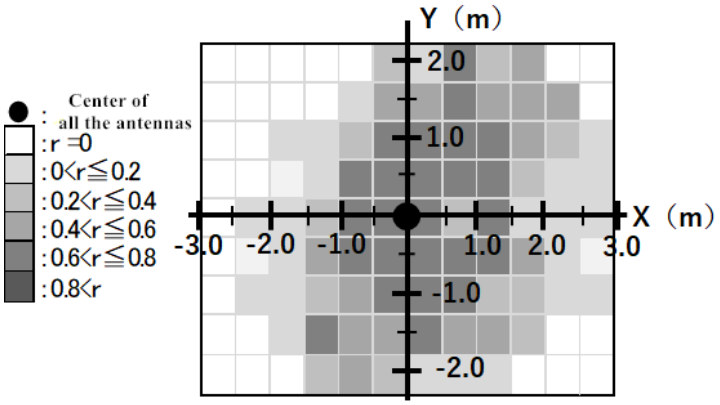

Figure 2-7　Average value of reading rates got by all the tags

2.4.3　Estimating position of a stationary object

In this study, a stationary object at the height of 1m above the floor is selected to check the position estimation accuracy. In order to improve reading rates, three tags were attached to the object at the height of 0.9 m, 1 m, 1.1 m. Then the object was moved to every measurement point, and when the object was placed on a measurement point, reading rates of all the antennas would be measured .

(1)　Obtaining reading rates

Number of variables used in the estamiton model would be increased when there were radio waves with different radio frequencies, which could improve goodness of fit using these training, but there was also a possibility of over-learning while using too many different radio frequencies. Therefore, two different radio output levels were used in this experiment and their power value were 30 dBm and 29 dBm.

Measurement of reading rates was repeated four times at all measurement points within the measurement area. The original coefficients for the three tags were $\omega_1 = \omega_2 = \omega_3 = 1/3$, and an average reading rate was calculated for each antenna at every measurment point. Since the number of antennas was 11 and the number of radio ouput levels was 2, the input vector was 22-dimensional and a dataset D of 468 (=117×4) sets for all the measurement points was obtained. Measurement time of the reading rate at each of the measurment point was 10 sec.

(2) Selecting estimation model

The dataset D was used by different candidate estimation models, including linear discriminant function, decision tree model, k-nearest neighbor algorithm, and neural network, and estimation performance of these models was compared. While using decision tree model, Gini Coefficient was used to represent the diversity index of node branching. While using neural network model, four layer neural network was constructed, including an input layer, two middle layers, and an output layer, and the number of nodes was 22, 11, 6, and 13 respectively for the mentioned four layers. The transfer function of the middle layers was two sigmoid functions, whereas the transfer function of the output layer was a linear function. K-fold cross-validation method was used to check performance of the candidate estimation models, and the obtained generalization errors for all the models were listed in Table 1 when number of groups K was defined as 12. According to Table 2-1, k-nearest neighbor algorithm method was selected to be the estimation model since its generalization error was the smallest.

Table 2-1 Generalization error of each model for stationary objects

Estimation Model	**Generalizaiton Error**
linear discriminant function	4.20
decision tree	1.75
k-nearest neighbor algorithm	1.57
neural network	1.86

(3) Modifying weighting coefficients

Using the estimation method selected in the previous section, an invector $\vec{w}^*$, set of all the weighting coefficients, was then calculated by Eq. (2.9) to make sure it is most fittable for dataset D, and the result was as follows: $w_1 = 0.27$, $w_2 = 0.17$, $w_3 = 0.56$. These values were the corrected weighting coefficients, and then the control variable of k-nearest neighbor model would be recalculated to find a best model for data set D. The position estimation model for a stationary object was determined as described above.

(4) Position estimation accuracy for the stationary object

After measuring reading rates at all the measurement points, position of the stationary object was estimated by the selected k-nearest neighbor model using the obtained reading rates. The position estimation result is shown in Figure 2-8. The average value of estimation errors was 0.02 m, while the standard deviation was 0.004 m, and the maximum value was 1.0 m. As shown in Figure 2-8, estimation error occurred at four points, which were marked by circles. The radius of the circle was proportional to the value of estimation error. And there was a place where estimation error was larger than 1.0m.

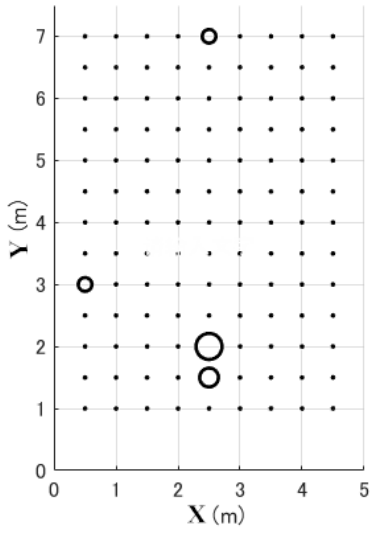

Figure 2-8 Estimation result of stationary objects

2.4.4 Estimating height of stationary objects

(1) Obtaining reading rates

Accuracy for height judgment of an object was examined through a test using two objects with different heights of 0.2 m and 1.0 m. The 0.2 m high object was attached with 3 tags at the height of 0.1 m，0.2 m，0.3 m from the floor, whereas the 1.0m high object was attached with 3 tags at the height of 0.9 m，1.0 m，1.1 m from the floor. At the 117 measurement points within the measurement range, reading rates of each antenna were measured for all the tags attached to the objects of different heights.

(2) Selecting model for height estimation

Estimation performance of linear discriminant function, decision tree, k-nearest neighbor model and neural network was compared using the newly obtained dataset, which was consisted of 936 (=117 × 2 × 4) sets. The generalization errors of all the models calculated by K-fold cross-validation method are shown in Table 2-2. When the division number K was set to 12, the generalization errors of all the models were 0.00. Therefore, k-nearest neighbor model used in section 2.4.3 was also chosen as the estimation model here for height estimation.

(3) Estimating the heights of stationary objects

Reading rates of each antenna for the two objects were newly measured at the 117 measurement points, a new dataset were obtained for verifying the estimation accuracy of height. After that, the dataset would be substituted in the selected k-nearest neighbor model. As a result, the height of the two objects were both estimated correctly at all the 117 measurement points, and the estimation error was 0.

Table 2-2 Generalization error of each model for height estimation

Estimation Model	Generalizaiton Error
Linear discriminant function	0.00
Decision tree	0.00
K-nearest neighbor algorithm	0.00
Neural network	0.00

2.4.5 Measuring flow line of a moving objects

Similarly to the experiment in Section 2.4.2, a worker is also defined as the measurement object in this experiment, and three tags were attached to the worker at the height of 0.15 m, 1.0 m, and 1.5 m acordding to the height of the worker's feet, waist and head.

(1) Obtaining reading rates

As mentioned before, there was no enough time for measuring reading rates while using multi radio wave frequecies, which means it is not suitable for flow line measurement. Consequently, radio wave used for flow line measurement should be transmited at a same power, and here in this experiment it was 29 dBm. The worker moved across all the measurement points, and the experiment was repeated four times for measuring reading rates.

(2) Selecting position estimation model

Reading rates of each antenna at a measurement point could be represented by a 11-dimensional input vector $\bar{R} = (R_1, \cdots, R_{11})$, and a data set including 468 (=117×4) invectors was obtained in this experiment. Similarly, estimation performance of linear discriminant function, decision tree, k-nearest neighbor model and neural network was compared using the data set. While using neural network model, the number of nodes in each layer was designed respectively as 11, 17 and 1. When the division number K was set to 12, generalization errors of all the models obtained by K-fold cross-validation method were shown in Table 2-3, in which generalization error of

k-nearest neighbor model is the smallest.

(3) Measuring the flow line of moving object

The object moved for about 40 seconds across the measurement range shown in Figure 2-2, and reading rate of each antenna was measured per second. Besides, the object was photographed by a video camera during the movement, and distance between the object and the measurement point was also actually measured. Using k-nearest neighbor model selected in the previous section, 38 positions were obtained from estimation within 40 seconds.

(4) Correcting the estimation result

The moving average method shown in Eq. (2.9) and Eq. (2.10) was used for correction of the flow line estimation result obtained by k-nearest neighbor method. The number of terms m of moving average is determined as five, the corrected flow line estimated from reading rates and the actual measured flow line were shown in Figure 2-9. The indexes of the corrected position estimation error were as follows: the average value was 0.22 m, the standard deviation was 0.14 m, and the maximum value was 0.43 m.

(5) Estimation accuracy of flow line measurement

The experiment of the moving object described in 2.4.5(3) was repeated 5 times. The average indexes of the estimation error were as follows: the average value was 0.29 m, the standard deviation was 0.09 m, and the maximum value was 0.66 m.

Table 2-3 Generalization error of each model for moving objects

Estimation Model	**Generalizaiton Error**
linear discriminant function	4.06
decision tree	2.11
k-nearest neighbor algorithm	1.53
neural network	5.94

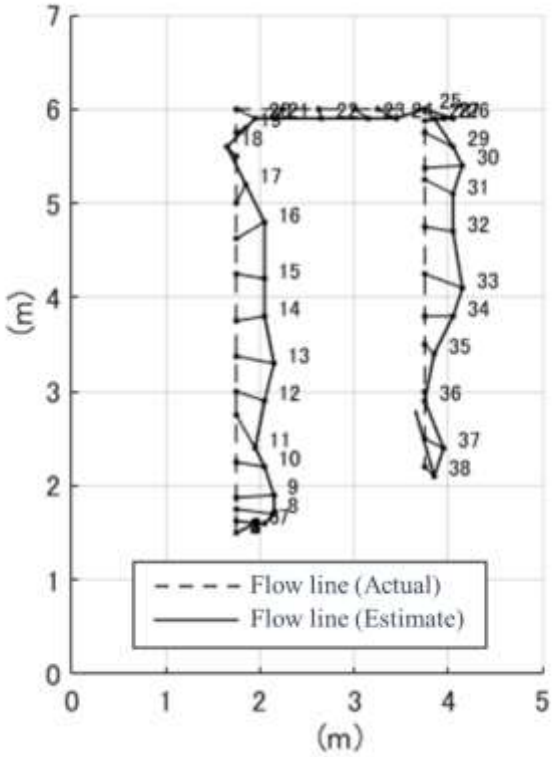

Figure 2-9 Estimation result of the flow line for moving objects

2.4.6 Discussion

Generally speaking, the average estimation error while using RFID is about one meters, and in previous studies under specific environments, the average estimation error can be lowered to about 0.5 m ~ 1.0 m. In our proposed method, although the maximum estimation error is 1.0m, the average estimation error for estimating stationary object is only 0.02 m, which is much lower than result obtained by previous studies.

Commonly, the standard of pallet used at production site is a square with a side length of 1.1m. Therefore, according to the measured estimation accuracy, the proposed method is appropriate for finding out mistakes in loading and unloading pallets by forklift or the other instruments. Furthermore, it is shown that heights of the two stationary objects with hieght difference of 80 cm can be estimated with an accuracy of 100%. Therefore, in this case the proposed method can be used for automating judgement of the hight of pallets.

While estimating a moving object's flow line using the proposed method, the maximum value of estimation error is 0.66 m. Since the safe distance between a worker and a mechanical equipment is 0.8 m according to JISB 9718, the maximum value of flow line estimation is acceptable. Based on the above results, the estimation accuracy of the proposed method is believed to be qualified to be used in a management system, which can automatically track flow line of a worker and check whether the worker is in the dangerous area around mechanical equipments for the production improvement and safety work. However, since the estimation error is not so minimized, the flow line measurement estimation of an object will be improved in the next chapter for productivity improvement .

Besides, the estimation model used in the application example was k-nearest neighbor model, which is selected according to the experiment environment and may not suitable in other cases. For different application environment, estimation model used in the system should be selected by appropriate testing method.

2.5 Conclusion

In the present study, a method is proposed for suppressing the interference of reflected radio waves for indoor positioning based on RFID.

Firstly, attaching several tags at different heights to a measurement object is proposed to decrease the influence of Null Point caused by radio interference, which could help to improve reading rates of the installed antennas. Then, reading rates of each antenna at different measurement points for all the tags are recorded while the masurement object was moving across the measurement area. After that, reading rate of an antenna at a measurement point is represented by a composite value combing the reading rates for all the tags at that point, which is the sum of reading rate for each tag multiplied by its calculated weight coefficient. At last, these composite values are used in an model to estimate position of the object, and the model is selected by comparing generalization error of different models for three kinds of measurements, including position estimation for a stationary object, height estimation for two

stationary objects ,and position estimation for a moving object.

The estimation accuracy is qualifed to find out the mistakes in loading and unloading pallets by forklifts. For the height estimation, since heights of the two stationary objects can be estimated correctly at all the measurement points, the proposed method can be used to judge top of an object is in the upper part or the lower part of the stacked shelves. According to the result of flow line measurement for a moving object, the average value of estimation error for the corrected positions is 0.22 m, and the maximum value is 0.43 m. In this case it is possible to develop a system for checking whether the worker is entering the dangerous area around mechinical equipments.

Reading rate was not measured in the area between two adjacent measurement points. Since the relationship between position of an object and the corresponding reading rate is nonlinear, the position estimation error for positions when an object is at a point which is not defined as measurement point may be higher than the result of the present study. Relationship of the estimation accuracy and the distance between adjacent measurement points should be studied in the future, and based on that size of the segment (distance between the adjacent measurement points) can be adjusted accoring to the estimation accuracy required in practice.

Chapter 3 A sensor system for work analysis automation

3.1 Introduction

This Chapter focuses on the development of a work analysis support system for distribution processing and presents a case study of work analysis at a retail clothing order fulfillment center. The system comprises ultrasonic sensors for measuring a worker's flow line and a smartphone for measuring the worker's dominant hand acceleration. Models for estimating the worker's motion were derived from the data obtained. Candidate estimation models were the statistical models linear discriminant function, decision tree, and k-nearest neighbor algorithm, and we used generalization error by cross-validation as an index for choosing the optimal estimation model. The system was applied to the example of analyzing order picking in a clothing distribution center. The κ coefficient obtained indicated the degree of matching between the results of video analysis and tracking by our system to be 0.6 or more, which confirmed the validity of our system.

3.2 Configuration of the Work Analysis Support System

Figure 3-1 shows the system proposed, which includes an ultrasonic sensor network, a smarphone, and a personal computer (PC). In Figure 3-1, the ultrasonic

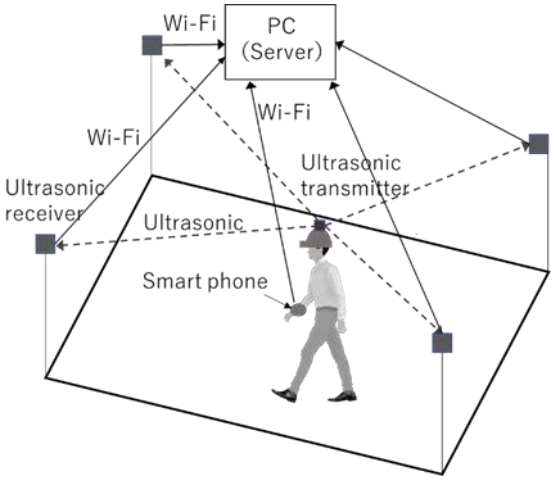

Figure 3-1 Structure of work analysis support system

network includes several receivers installed on indoor fixed structures wall and a transmitter attached to the worker. Here, the position of the transmitter is used as the position of the worker. The smartphone used in the system has a built-in acceleration sensor, and the smartphone and ultrasonic sensor are connected to the PC via a wireless local-area network (LAN). During data acquisition, the execution files for the ultrasonic sensors, smartphone, and work analysis are processed in parallel in the PC. Every time a receiver receives an ultrasonic wave, the time when the wave is transimitted and received are processed and recorded by the executable files of the ultrasonic sensor.

Then, the position of the transmitter is calculated and the data are recorded to the ROM of the PC. The executable file in the smartphone obtains the acceleration and transmits it for recording to the ROM. The work analysis module retrieves the data for position and acceleration to estimate the worker's motion. Although the ultrasonic sensors and smartphone write data to the ROM at different rates, the data retrieved from the ROM by the work analysis module are obtained at fixed time intervals to make sure that the position data are synchronized with the acceleration data.

3.3 Proposed Method

3.3.1 Measuring position using ultrasonic sensors

The position of the transmitter is calculated using the ultrasonic wave's arrival time from the transmitter to the receiver, and the calculation procedure is as follows. The trigger signal is transmitted from the PC to all of the transmitters and receivers, and then the transmitters send out pulse signals to their surroundings. For each receiver $p_k, (k = 1, \cdots, J)$, the time $t_k, (k = 1, \cdots, J)$ from the reception of the trigger signal to the arrival of the pulse signal from the transmitter is measured. Their position relation is represented as shown in Figure 3-2 .

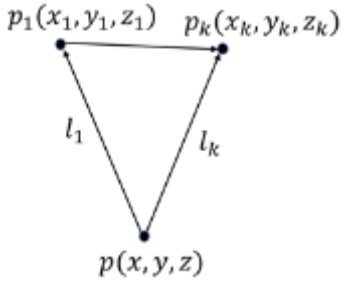

Figure 3-2 Positional relation of ultrasonic transmitters and receivers

If the speed of sound is assumed as c, then the distance l_k between the transmitter p and the receiver p_k is obtained using the following equation.

$$l_k = ct_k, (k = 1, \cdots, J) \tag{3.1}$$

Next, the position (x, y, z) of the transmitter p will be calculated. The position relationship of each receiver and transmitter is shown in Figure 3-2. Here, (x_1, y_1, z_1) is the position of the receiver p_1, (x_k, y_k, z_k) is the position of the receiver p_k, and (x, y, z) is the position of the transmitter p. The distance $l_{k,}, (k = 1, \cdots, J)$ from the transmitter to each receiver is calculated using equation (3.1). In Figure 3-2, the distance between the transmitter p and receiver p_1 can be obtained as follows:

$$l_1^2 = (x_1 - x)^2 + (y_1 - y)^2 + (z_1 - z)^2 \tag{3.2}$$

The distance from the transmitter p to any receiver p_k is expressed by:

$$l_k^2 = (x_k - x)^2 + (y_k - y)^2 + (z_k - z)^2 \tag{3.3}$$

By expanding the right-hand side of Eq. (4.2), the following equation can be obtained:

$$l_1^2 = x_1^2 - 2x_1x + x^2 + y_1^2 - 2y_1y + y^2 + z_1^2 - 2z_1z + z^2 \tag{3.4}$$

By expanding the right-hand side of Eq. (4.3), the following equation can be obtained.

$$l_k^2 = x_k^2 - 2x_kx + x^2 + y_k^2 - 2y_ky + y^2 + z_k^2 - 2z_kz + z^2 \tag{3.5}$$

Then, by subtracting Eq. (3.4) from Eq. (3.5), the following equation can be obtained rearranging terms:

$$2(x_k - x_1)x + 2(y_k - y_1)y + 2(z_k - z_1)z$$

$$= (x_k^2 + y_k^2 + z_k^2 - l_k^2) - (x_1^2 + y_1^2 + z_1^2 - l_1^2) \quad (3.6)$$

The collection of all the receivers is then as follows:

$$\begin{bmatrix} 2(x_2 - \mathrm{x}_1) & 2(y_2 - y_1) & 2(z_2 - z_1) \\ 2(x_3 - x_1) & 2(y_3 - y_1) & 2(z_3 - z_1) \\ & \vdots & \\ 2(x_J - x_1) & 2(y_J - y_1) & 2(z_J - z_1) \end{bmatrix} \begin{bmatrix} x \\ y \\ z \end{bmatrix}$$

$$= \begin{bmatrix} x_2^2 + y_2^2 + z_2^2 - l_2^2 - x_1^2 - y_1^2 - z_1^2 + l_1^2 \\ x_3^2 + y_3^2 + z_3^2 - l_3^2 - x_1^2 - y_1^2 - z_1^2 + l_1^2 \\ \vdots \\ x_J^2 + y_J^2 + z_J^2 - l_J^2 - x_1^2 - y_1^2 - z_1^2 + l_1^2 \end{bmatrix} \quad (3.7)$$

In matrix-vector notation, this can be written as follows:

$$AX = B \quad (3.8)$$

From Eq. (3.8), the position X of transmitter p is calculated using the following equation with the least squares method:

$$X = (A^T A)^{-1} A^{\mathrm{T}} B \quad (3.9)$$

In Eq. (3.7), it is assumed that the distance measured from each receiver to the transmitter is correct. Although different from radio waves, ultrasonic waves have the property of diffraction, which could help the receiver to receive ultrasonic waves generated by the transmitter even if the worker enters the shade of a pillar or a passage between the shelves. A measurement error may also occur in the situation that the time of flight (TOF) is not correct while measuring distance. Furthermore, there is the possibilities that the ultrasonic waves cannot be received by a receiver when the worker crouches to take out products from under shelves. In order to deal with the influence of wrongly measured distances caused by obstacles, this paper used a way of sequentially selecting receivers for position estimation. This method is a specialized way for distribution centers. In Figure 3-3, three receivers are used for estimating the transmitter's position but not that of the receiver p_n because the distance measured by receiver p_n is not correct. The wrongly measured distance l_n

should not be used to estimate transmitter position, or the estimation error will be too large. Therefore, a method of sequentially selecting receivers for position estimation is proposed to prevent large estimation error. The k-th position is estimated by estimating the distance of receiver p_1, p_2, p_i, and p_n can be any other receiver. The measurement error d_i is defined as the difference between the actual distance r_i and estimated distance l_i when using receiver p_i for estimation. All the other receivers are used to determine the value corresponding to measurement error, and then values of those errors are arranged from small to big, which is presented by $(d_{k1}, d_{k2}, \cdots, d_{kn}), (d_{ku} < d_{ku+1}, u = 1,2, \cdots, n-1)$. The three receivers with smaller measurement error (d_{k1}, d_{k2}, d_{k3}) are selected to estimate the $(k+1)$th position p^{k+1} on the flow line. In this paper, the method described above is used to prevent the influence of obstacles on the estimation accuracy in logistics centers.

Eq. (3.7) shows how to use the three receivers with smaller error to estimate the transmitter's position. However, if there are only two receivers not affected by obstacles, the estimation error of the transmitter's position obtained by Eq. (3.7) will be too large. In this case, the transmitter's position will be recalculated by obtaining the intersection point of the two circles, which are drawn with a radius using the distance measured from each sensor to the transmitter. Since it is a geometrical problem to obtain the intersection point of the two circles, the detailed process is omitted due to space limitations. In order to determine whether to select three receivers or two for position estimation, the normal-pace walking speed of the MTM method is considered. The normal speed is about 1.33 m/sec, and in this study the threshold value is set to 3.0 m/sec. When using three receivers, if the speed got by the distance between two adjacent estimated positions divided by the measurement time is equal to or higher than the threshold, the position of the transmitter will be recalculated using two receivers. Furthermore, the possibility that only or less than one receiver is not influenced by obstacles in the measurement distance also existed. In this situation the position of the transmitter cannot be estimated. In this case, after obtaining the flow line using the above procedures, 100 position data obtained in 1

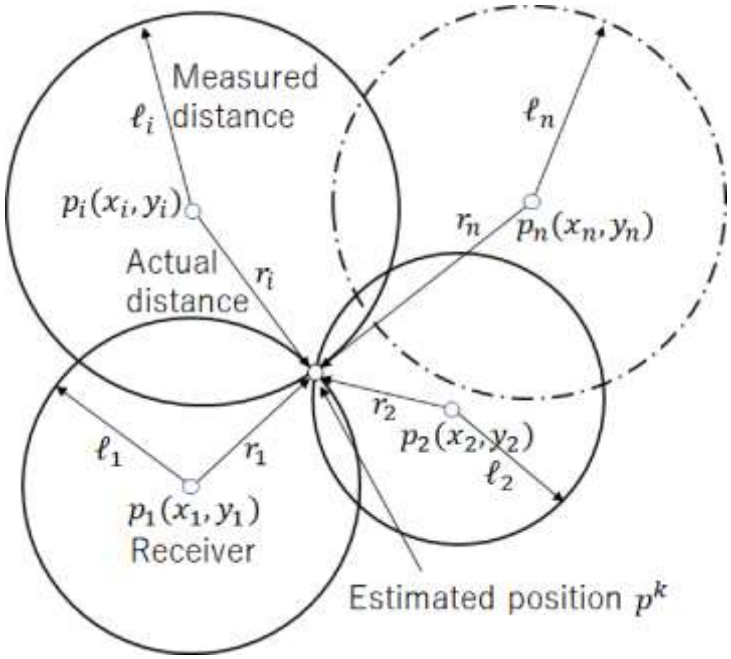

Figure 3-3 Measured distances of receivers

sec will be used as the median for correcting the flow line.

3.3.2 Estimating type of motions using ultrasonic sensors and an acceleration sensor

The position data of the worker and the acceleration data of the dominant hand are obtained from the ROM of the PC at fixed time intervals. The moving speed is calculated using the distance between consecutive position data points for the worker. To estimate the type of worker motion, information about position, moving speed and its changes, and the acceleration of the worker's dominant hand are used.

It is assumed that the running time of this system for work analysis is in the range of 0.5 to 8 hr. If the number of data acquired per second is too large, then there is a danger of exceeding the memory upper limit of the PC and corrupting all the data accumulated during the work analysis. Conversely, if the number is too small, then the risk of missing an operation performed over a short time increases. Thus, it is important to set an appropriate number of data acquisitions per second according to the time needed for work analysis.

After acquisition of both worker position and hand acceleration data, the estimation model used to estimate the types for motion needs to be determined. These motions are divided to two types: (1) moving operation in which the worker is only walking and (2) main work operation, including picking, inspecting, packing, or loading items to a dolly. First, the speed of the moving operation is higher than that of the main work operation. Second, the location is different for different kinds of main work operations, such as picking, packing, and loading items to a dolly. Additionally, the acceleration of the dominant hand is believed to be higher when the worker is doing a main work operation rather than moving. These differences are used to distinguish motions. In this study, the output value of the estimation model is defined as different values for different types of operation; for example, the moving operation is defined as 1, the loading to a dolly operation is 2 and the picking operation is 3.

It is assumed that the relationship between the input data and output value is linear or nonlinear. If the relationship is linear, a linear discriminant function is used as the estimation model. If it is nonlinear, a decision tree, k-nearest neighbor algorithm, or some other method is considered. Next, the generalization error obtained by the k-division cross-validation method is used as an index for evaluating the estimation performance of these candidate models [10]. The moving operation and main work operation are performed in advance to acquire the data representing the correspondence between the input data and output values. If the number of variables of input data is indicated as N, then the data can be represented by a N-dimensional input vector $\vec{r} = (r_1, \cdots, r_N)^T$. The output value is defined as $y \epsilon R$. The total number of input/output pairs is indicated as M, and the ith input/output value pair is denoted by $(\vec{r}_i, y_i)$. If the control variable $\vec{\omega}$, and the estimation model variable θ are defined, then the estimation model for the input/output pair can be expressed as follows:

$$y = f(\vec{x}, \vec{\omega}, \theta) \tag{3.10}$$

For example, when the estimation model variable θ represents the decision tree model, the elements of the control variable $\vec{\omega}$ are the branching conditions (features such as moving speed and threshold) of the nodes in the classification tree. The

collection of input/output pairs is represented by dataset $D = \{(\vec{r}_1, y_1), \cdots (\vec{r}_M, y_M)\}$. Data set D is divided equally into K groups, and the uth test set is $C_u, (u = 1, \cdots K)$. If the test set C_u is removed from data set D, we can obtain the training data set, $L_u (= D \backslash \mathrm{C}_u)$. The training data set is used to obtain the control variable of the estimation model. The test set is used for assessment of the generalization error of the final chosen model once the control variable is determined. The generalization error $A(\theta)$ obtained by the K-fold cross-validation method is expressed as follows:

$$A(\theta) = \frac{1}{2} \sum_{u=1}^{K} \sum_{(\vec{r}, y) \in C_u} (y - f(\vec{r}, \vec{\omega}_u^*, \theta))^2 \qquad (3.11)$$

The data set is divided into a training set and a test set to calculate $A(\theta)$. Using $f(\vec{r}, \vec{\omega}_u^*, \theta)$, which uses the best-fitting control variable $\vec{\omega}_u^*$, for training set L_u, the performance of the estimation model can be asymptotically evaluated if we can accurately determine whether or not the test data are properly associated with the training data. Then, the model with the smallest generalization error $A(\theta)$ is selected as the estimation model. The estimation model is determined using the above procedures. Once the estimation model is determined, newly input data are analyzed to identify the motion in real time.

Using the method mentioned above, a support system for real-time work analysis can be constructed. The writing speed for the data from the ultrasonic sensor to the ROM is 30 times per second, while the speed is 10 times per second for writing data from the smartphone to the ROM. The work analysis module retrieves the position and acceleration data simultaneously from the ROM at intervals of 0.5 seconds. The ultrasonic sensors and smartphones are commercially available, so the total cost of the system was less than ¥200,000. The ultrasonic sensor beacon manufactured by Marvelmind was used in our system, and each sensor can transmit and receive ultrasonic waves throughout a hemisphere with a radius of 30m to ensure the distance between sensors can be measured at 30Hz.

3.4 Application Example

3.4.1 Introduction of application background

The system developed was used in a logistics center for retail clothing order fulfillment, and the results obtained using the system was compared with the result obtained using video analysis.

The ultrasonic sensors used in this experiment were limited to a maximum receive distance of 30 m. Therefore, it was difficult to set the entire floor as the measurement area, and in this study a concentrated area for distribution work was considered. Since picking work was mainly done within a range of $16\ \mathrm{m} \times 16\ \mathrm{m}$, the area for picking seasonal products was selected to be the measurement area. In preliminary survey, workers were sometimes walked out of the measurement area, but its case was excluded from the analysis considering the low frequency and the limitation of the maximum receiving distance of ultrasonic sensors.

The shelves were placed in two rows of nine stacks, and the height of each shelf stack was 1.6 m. The picking methods included both single picking and a total picking, and the shipment volume for total picking was much more than that for single picking. Therefore, the work analysis in our experiment was based on total picking operations. For the installation of the receivers, the area was divided into four sections and there were no pillars in each section. At least three receivers were set for each section to make sure that ultrasonic waves could be received by three or more receivers. The positions for all of the ultrasonic sensors (shown in Figure 3-4) were determined by a preliminary experiment to ensure that it could be used for flow line measurement. A total of 10 receivers were set up for the entire experimental area.

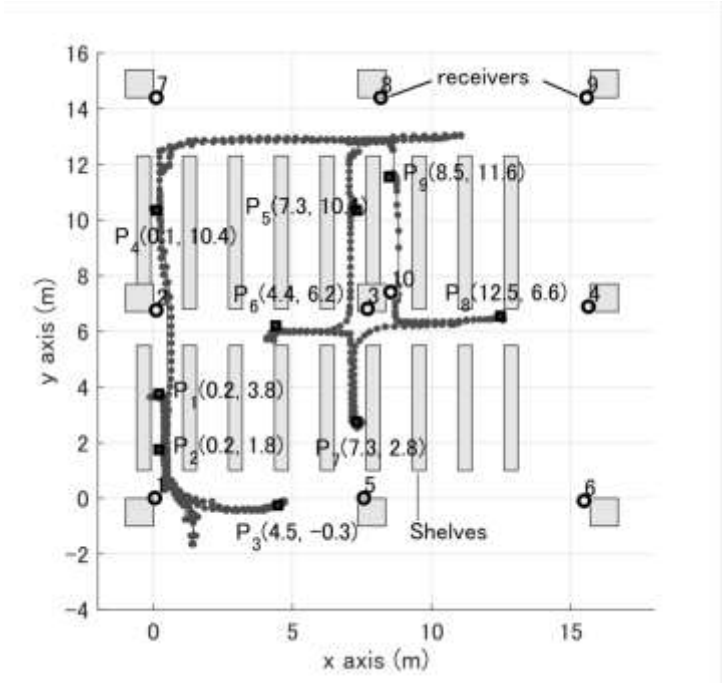

Figure 3-4 Measurement points and locus of a worker

The worker participating in the experiment was a female leader with one year of experience. The experiment and its purpose were explained to the worker participated in the experiment, and she understood that the experiment might be interrupted or canceled at any time. Moreover, the worker was told that personal information, such as name and age, would not be released, and that the measurement data would be used only in the context of this study. After that, the experiment was started.

3.4.2 Position measurement accuracy

The accuracy of position measurement with the ultrasonic sensors was verified. In the measurement area, 10 ultrasonic receivers were installed on the sides of nine structural columns at a height of 3.2 m from the floor. As mentioned above, 30 distance data points were acquired per second by the ultrasonic receiver, and the position of the ultrasonic transmitter was calculated using Eq. (4.9). Nine measurement points $(P_1, \cdots, P_9)$were defined in the area, and the coordinates for each point are shown in Figure 3-4.

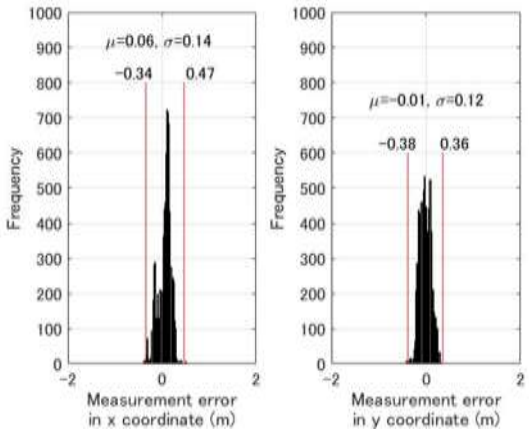

Figure 3-5 Measurement error for (left) x coordinates and (right) y coordinates

The values of the coordinates were measured using a measuring tape for use as the actual values. During the verification experiment, the worker walked back and forth between the measurement points and stopped for 30 sec when she was closest to each measurement point. In this way, when the movement speed was lower than 0.2m/sec, the worker was judged as having reached the measurement point. The worker's flow line during the experiment is also shown in Figure 3-4. A total of 7,823 positon data points were obtained from the nine measurement points. The measurement error was defined as the differences between position data obtained using ultrasonic measurement and tape measurement. The left panel of Figure 3-5 shows the distribution of the measurement error of the x coordinate values for all of the position data, while the right panel shows that of the y coordinate values. The average value of the measurement error was 0.05 for the x coordinate values, and since the standard deviation was $\sigma = 0.11$m, the interval of $\pm 3\sigma$ was (-0.29, 0.39) m. For the y coordinate values, the average value of the measurement error was -0.01 m, and since the standard deviation was $\sigma = 0.11$ m, the interval $\pm 3\sigma$ was (-0.35, 0.33) m. In this study, the accuracy of the system proposed was tested in a measurement range of $20\text{ m} \times 20\text{ m}$. There was 10 receivers installed, and the average value of measurement error was about 0.15 m (deviation ± 0.06), while the maximum value was about 0.33 m.

The accuracy of flow line measurement using the conventional RFID system has

been reported [69]. When there were 10 antennas in a measurement range of $7\ \mathrm{m} \times 5\ \mathrm{m}$, the average value of measurement error was about 0.29 m (Standard deviation $\pm 0.14\ \mathrm{m}$), while the maximum value was 0.66 m. Accordingly, the results of ultrasonic sensor method were better than those of the RFID system.

Acceleration sensors were used in a motion capture device for flow line measurement [70]. When the measurement range was $16\ \mathrm{m} \times 30\ \mathrm{m}$, the measurement error was 0.45 m (Standard deviation $\pm 0.23\ \mathrm{m}$) in x axis and 0.27 m in y axis when the worker moved in a rectangular path; this was also larger than the values obtained using ultrasonic sensors. Additionally, although there is no specific numerical value, it is believed that the measurement error is accumulated every time the direction of the acceleration sensor changes while moving. In distribution centers, a worker's direction of movement usually changes frequently, which can result in very large measurement error during flow line measurement.

3.4.3 Video analysis

The worker's motion while she picked a batch of items was recorded using a video camera, and the records were used for work analysis. The moving operation comprises the motion of walking while pushing a hand cart and walking from the cart to a shelf. The picking operation is the motion of picking items from a shelf, which includes reaching for an item with a hand, grasping the item, and checking the item using a "handy" terminal. When items picked by hand reached the required quantity, the worker walks back to the hand cart to put the items in folding containers; these actions are collectively called dolly operation. Placing items in containers includes actions such as arranging the items and changing the order of the containers. The time ratio of each operation determined from video recordings is shown in Figure 3-6. For the time ratios of picking a batch of items, the moving operation, dolly operation, and picking operation were respectively 43%, 10%, and 47%.

Figure 3-6 Time ratio of each operation by video analysis

3.4.4 Worker's flow line

During the process of picking a batch of items, the worker's flow line was also measured by the support system while the video camera was recording the process. The worker's flow line measured using the conventional method is shown in Figure 3-7. The number of items in one batch was 89, but 23 of them were non-seasonal items, so the worker had to walk out of the measurement area while picking these and these motions were not used in the work analysis.

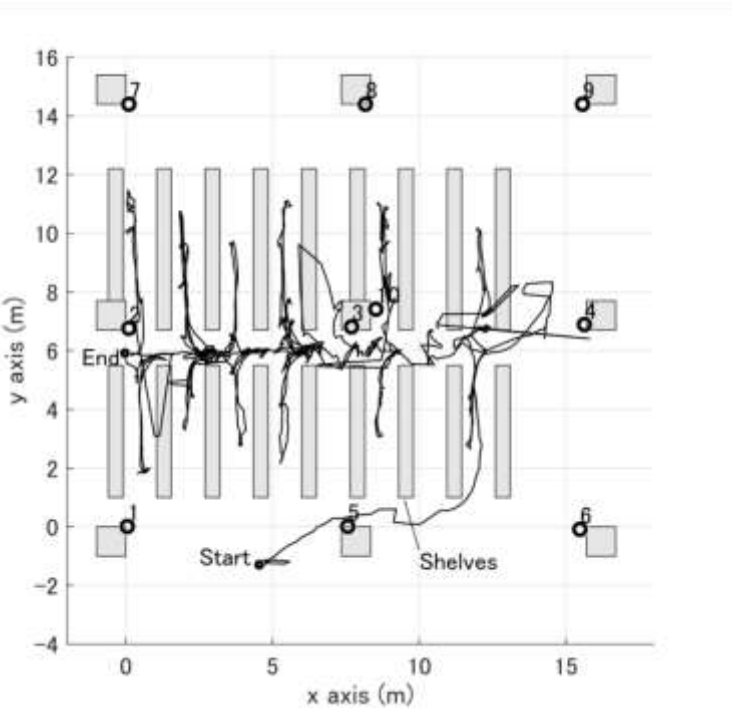

Figure 3-7 Worker's flow line while picking items for one batch (conventional method)

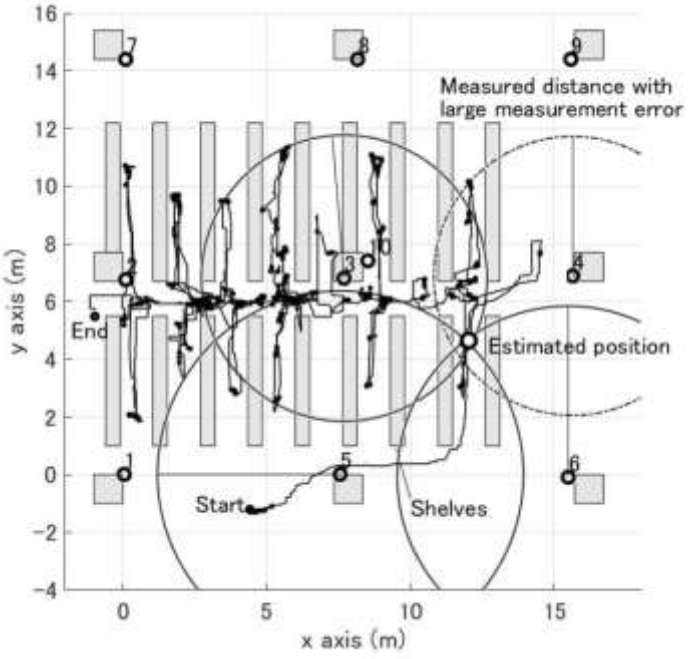

Figure 3-8 Worker's flow line measured using the method proposed

In order to deal with the distance measurement error caused by small ultrasonic diffraction, this paper uses a method of sequentially selecting receivers to estimate the transmitter's position. Figure 3-8 shows an example of a transmitter's position estimation process. The numbers of the three receivers with smaller distance measurement error are 3, 5, and 6. A circle is drawn with the distance measured as the radius for each receiver. The intersection point of the three circles is estimated to be the transmitter's position. A dotted circle is also drawn for sensor 4, where there is a large measurement error for the distance. According to the distance measured obtained in the next circle (1/100 sec later), the position of the worker is estimated using the three receivers mentioned above.

For the accuracy of worker detection by ultrasonic sensors, results obtained by the basic method presented by Eq. (3.7) and the above added method have been compared. The ultrasonic sensors used in this paper measured the distance from all of the receivers to the transmitter at 100Hz. Figure 3-7 shows the result of flow line measurement obtained using the conventional method presented by Eq. (3.7), and Figure 3-8 shows the results using the method added, that of sequentially selecting

receivers.

Overall, the flow line could be identified correctly by both methods when the worker walks through the passage between commodity shelves. However, there is measurement error when using the conventional method in other situations. In Figure 3-7, the flow line changes greatly near receiver 3, and visually the worker was in the area where commodity shelves are located and flow line measurement error was identified. There is also an area where the flow line stretches toward receiver 4. According to film analysis, the worker was taking items from the shelf and then loading them onto the dolly. The conventional method is not appropriate to analyze those motions. In Figure 3-8, it can be confirmed from the flow line that the worker moved around several times from the front to the backside of the dolly at a position near receiver 3. Comparing to the results of the conventional method shown in Figure 3-8, the method proposed can measure the flow line correctly when the worker is picking products and loading them to the dolly.

The total distance of the intervals with a moving speed more than 0.2m/sec was 199.3 m, and the average speed was 0.7 m/sec. The moving speed was 1.58m/sec when using MTM. The reason why the average value of the moving speed was lower than the speed obtained using MTM is that the worker was performing picking operations while moving the hand cart. However, when the worker was walking away from the hand cart, several positions with a speed higher than 1.58 m/sec were identified. According to the video analysis described in Section 3.2, the picking operation was implanted at 50 positions at the shelves. The number of items taken from each shelf was from one to five. There were 23 points where the moving speed was lower than 0.2 m/sec in front of the shelves (black circles); the values of the y coordinates were all 6 m and the route was parallel to the x axis. This is believed to be repeated motions of loading items onto the dolly and pushing it. Thus, when the moving speed was higher than 0.2 m/sec for almost half of the 50 positions where the picking operations occurred, it is difficult to calculate the picking position and the picking time using only the moving speed.

3.4.5 Selection of estimation model

Next, a motion estimation model for automating the work analysis was developed, and the four variables described in Section 3.3.2 were considered for use. Additionally, the flow line and acceleration of the dominant hand were used as input variables, which were measured during the above process of picking a batch of items. The input data was obtained at intervals of 0. 5 sec, and were used to calculate the output value applying the method described in Section 3.3.2 and worker motion datasets were obtained. Using these datasets, the estimation performance of linear discriminant function, decision tree, neural network and k-nearest neighbor algorithm were compared. The Gini coefficient was used for node branching in the decision tree model. When the division number of data set K was set to five, the generalization errors of the three models were calculated as follows: linear discriminant function 0.28, decision tree 0.27, neural network 0.30, and k-nearest neighbor algorithm 0.25. Although there was no significant difference for the generalization error of the three models, the value was minimized while using k-nearest neighbor algorithm, and it was selected for motion estimation in this case.

3.4.6 Performance of the estimation model

This section shows the estimation performance using the k-nearest neighbor algorithm. Datasets were divided into five groups, as described in Section 3.4.4. Datasets from groups 2 -5 were used as training sets for determining the best-fitting control variable of the k-nearest neighbor algorithm. Next, an estimation was executed using k-nearest neighbor algorithm and the data set of Group 1. The same values obtained using estimation model using one data set and the actual values analyzed by the video analysis are shown in Table 3-2. The number of data points in Group 1 is 189. According to the film analysis shown in Figure 3-9, the time ratios of moving operation, dolly operation and picking operation were 44%, 10%, and 46%, respectively. Correspondingly, the results using the k-nearest neighbor algorithm were 43%, 10%, and 47%, as shown in Figure 3-10.

The kappa coefficient proposed by Cohen [71] has been widely used to describe the association between categorical variables, and it can be thought of as a correlation coefficient describing the relation or shared variance between two categorical-level variables [72]. The Kappa statistic varies from -1 to 1, and the most widely accepted correlation between kappa statistic and strength of agreement is proposed by Landis and Koch [73], and the relationship is shown in Table 3-1. In which, a kappa in the range of 0.61-0.80 is considered ‘substantial’ agreement.

In the present study, the k coefficient is 0.66, and so the relationship between the result obtained by video analysis and the result obtained by proposed estimation model is believed to be ‘substantial’, which means a high degree of consistency. Accordingly, the result is the thesis is believed k to be “acceptable”. Based on the results, the work analysis performance of this system was tested by the degree of agreement with the actual values, and the results indicated that the system was practical.

Table 3-1 Correlation of Kappa Statistic and Strength of Agreement

Kappa Statistic	Strength of Agreement
< 0.00	Poor
0.00-0.20	Slight
0.21-0.40	Fair
0.41-0.60	Moderate
0.61-0.80	Substantial
0.81-1.00	Almost Perfect

Table 3-2 Estimation performance of the estimation model (Number of data points in Group 1)

		Estimation Model			
		Moving	Dolly	Picking	Total
Film Analysis	Moving	64	4	16	84
	Dolly	2	16	1	19
	Picking	15	0	71	86
	Total	81	20	88	189

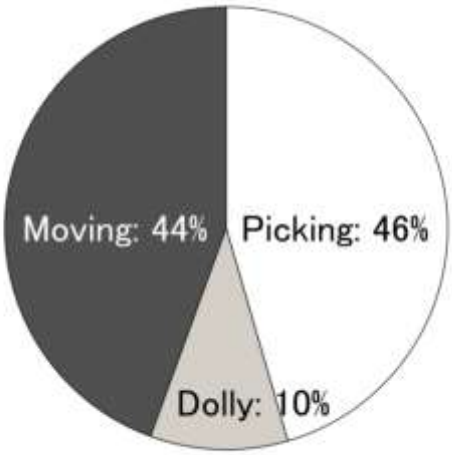

Figure 3-9 Time ratio of each operation determined by video analysis of dataset 1

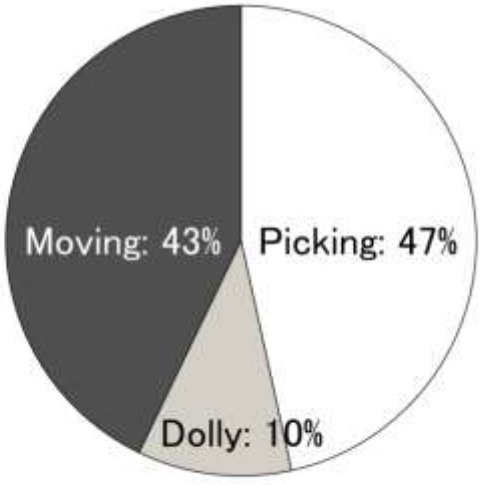

Figure 3-10 Time ratio of each operation estimated using the k-nearest neighbor algorithm and the dataset of Group 1

3.4.7 Discussion

This study proposed a method that uses a combination of ultrasonic sensors and acceleration sensors to establish a system for work analysis automation without using information from the existing production management system. In distribution centers, there are many obstacles such as shelves and pillars, and the estimation error is too large to estimate the position when using the TOF method. Accordingly, estimation accuracy was improved using the method proposed here; that is, sequentially selecting receivers to estimate the position of the transmitter. Furthermore, the accuracy of motion estimation using the acceleration of a worker's dominant hand has been proven effective after comparing results obtained applying video analysis. Finally, the problem of obstacles being present is eliminated using the system proposed. For practical use of this system, if a standard time for each motion is set, it is believed to be possible to analyze the deviation between the duties assigned to individual employees and the duties actually carried out, to compare the difference between skilled and unskilled workers, and to manage every worker's picking task history.

Because this system used ultrasonic transmitters marked with identifiers, it was possible to trace the flow line of a specific worker. Furthermore, the system processing time required to display the flow line and calculate the moving distance or time ratio was less than five seconds. Additionally, there was no interference in the supervisor's work or the work of others at the work site when the system was used for work analysis.

Accordingly, to the characteristics of logistics centers, besides flow line measurement accuracy, there are also other qualitative requirements. The advantages of this system are described as follows. As mentioned above, the existence of many visual obstacles is one of the most prominent characteristic of logistics centers, and this has a close relationship with flow line accuracy. Frequent change in the site layout is another prominent characteristic of logistic centers. Since clothes are usually classified by seasons, the storage layout changes frequently. It is not unusual that

these clothes are replaced by other products such as miscellaneous goods, or office equipment. Therefore, installation position of measuring equipment should be easy to change. Antennas used for RFID method need to be placed on the ceiling and require installation, and cameras used for image processing need to be installed at appropriate heights. Since ultrasonic sensors do not require special installation, they are more suitable for logistics centers.

While using RFID for flow line measurement in Chapter 2, the average estimation error is 0.29 m, and the maximum estimation error is about 0.66 m, and the average estimation error is about 0.3 m when using acceleration sensor or RFID or Image processing in previous studies. In chapter 3, the average measurement error is 0.15 m and the maximum measurement error was about 0.33 m using the proposed system, which are almost half of the previous values. Moreover, the estimation accuracy while using ultrasonic wave was almost close to the estimation results while using Ultra Wideband (UWB) which cost much more than using the proposed two methods.

From the viewpoint of choosing this system as an initial investment cost, it is also better than RFID method and image processing method. In addition, depending on the distribution center and the level of work experience, different workers spend different amounts of time doing the same work. In order to investigate the difference of work time for different workers, it is necessary to investigate time required for each kind of motion, such as picking products or walking. Motion capture devices are believed to be better for work time measurement. However, when wearing the device while working, it is harder for a worker to perform tasks, which makes it hard for ordinary use. In this study, an estimation method based on the position of a worker and the acceleration of her dominant hand is used to estimate the work time for each kind of motion. In this system, an ultrasonic sensor is attached to the worker's helmet, and an acceleration sensor is attached to her dominant arm. From the viewpoint of alleviating work interference, it is conceivable that this system is better than using motion capture devices.

In terms of academic limitations, to date there has been no research performed to

reduce position estimation error caused by obstacles. The wavelength of radio waves is long enough to be received in an environment where there are many obstacles. But for ultrasonic waves, the characteristic shorter wave-length reduces the possibility of receiving diffracted waves by receivers. In order to resolve this problem, it is an important task to develop a control circuit that dramatically increases the reception sensitivity of ultrasonic waves. In terms of practical application limitations, the system was developed by researchers of an organization having no actual association with the distribution center. If the information describing work carried out in the distribution center was more detailed, such as product name, picking time and location in the center from which it is collected, the work analysis itself should be more accurate. Moreover, it is hard to integrate a system developed by external organizations such as universities to an existing production management system in a short period of time.

The system introduced here has been developed to enable quick work analysis, doing so with an accuracy equal to or higher than that of video analysis. In the future, there will be further research, for example, setting a standard work time for a task, distinguishing gaps between the duties assigned to a worker and the duties actually carried out, comparing skilled and unskilled workers, and managing every worker's picking task history.

3.5 Conclusion

In this study, a support system was developed for automating the work analysis of distribution processing. In logistics centers, the items to be picked and shipped change frequently, so it is necessary to promptly obtain work analysis results for improving efficiency. There is also a need to transfer the mission of work analysis from industrial engineering experts to on-site supervisors or small worker groups. Therefore, this research was designed to solve these problems.

Ultrasonic sensors were used to measure the worker's flow line, and analyze worker travel distance and speed. In addition, using moving speed and dominant hand

acceleration as input data, the type of motion, such as moving or picking operation, could be estimated with a model determined using a cross-validation method.

A work analysis experiment using the system developed was conducted in a logistics center for retail clothing order fulfillment. The flow line and moving speed of the worker were calculated. Moreover, the degree of agreement between the estimated results obtained by the system and the actual motions determined using video analysis revealed a coefficient higher than 0.6, verifying that the results are acceptable.

Furthermore, at the logistics center, it is necessary for the workers in charge of the site to use the system easily and constantly. Plans for the system developed include further practical use for analyzing the differences in supervisory jobs and those of other workers, including regular and temporary employees, to satisfy the objective of ‘same labor, same wage’.

Chapter 4 A Sensor System for Counting Stacked Plywood Sheets

4.1 Introduction

Two methods and an apparatus are proposed for counting stacked plywood sheets in this chapter. The first method is based on the normalized cross-correlation method. In this method, an inspection image is first scanned and the cross-correlation of the template image of the stacked plywood cross-section is then investigated in order to obtain the number of normalized cross-correlation maxima, which indicates the number of plywood sheets. The second method is based on the cross-validation method and uses an estimation model to determine the central portion of each plywood sheet in the cross-section of the plywood stack. An application example demonstrates that the methods proposed can reduce the time required for counting plywood sheets by more than 40% as compared to current methods.

4.2 The Characteristics of Stacked Plywood Sheets

For the situation in which the difference in gradation of the brightness of the plywood cross-section is large, in choosing a measurement method, the emphasis is on simplification. As such, the NCC method should be used to measure the number of plywood sheets. When it is difficult to accurately determine the number of plywood sheets using the NCC method, the proposed estimation model method should emphasize measurement precision.

In the present study, the measurement object is common plywood. An example of the inspection task is shown in Figure 4-1. The stack contains 500 plywood sheets, and two workers are tasked with determining the number of the sheets by visual inspection. It takes one worker approximately four minutes to count 500 plywood sheets one time, and confirmation is achieved by repeated counting until the numbers reported by the two workers are the same.

Figure 4-1 Counting stacked plywood sheets

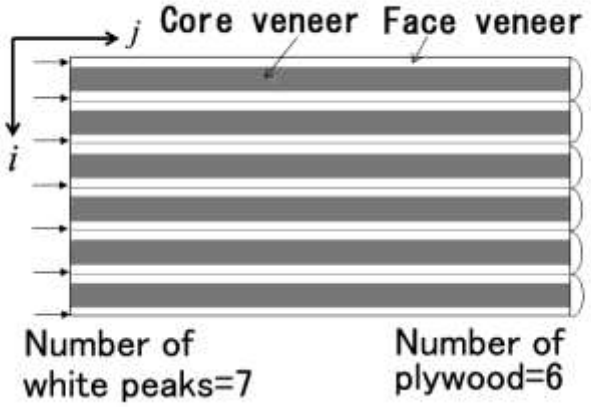

Figure 4-2 A schematic diagram of the stacked plywood sheets

A schematic diagram of stacked plywood sheets is shown in Figure 4-2. The color of the central portion (core veneer) and the top and bottom ends (face veneer) of a plywood sheet are different, which is a result of the plywood sheet manufacturing process which is presented by Japan Wood-Products Information and Research Center. In Figure 4-2, the arrows indicate gaps between plywood sheets. The purpose of the present study is to measure the number of plywood sheets using the color gradations of the cross-sections.

4.3 Comparative and Proposed Method

4.3.1 Apparatus configuration

The architecture of the apparatus is shown in Figure 4-3. In the coordinate system, the tangential direction of the stacked plywood sheets is defined as the X axis, the sagittal plane is defined as the Y axis, and the normal direction is defined as the Z axis. The stand base contains an AC servomotor ②, a servomotor control device ③, a programmable logic controller (PLC) ④, an analog input/output unit ⑤, a support pillar ⑥, and other equipment. A vertical rail is attached to the line sensor camera ①, and holding the rail with the roller bearings suppresses lateral blurring as the camera rises. A wire winding drum is attached to the servomotor. The camera is suspended by a wire with a diameter of 2 mm via a pulley at the upper part of the column, and through normal rotation of the motor, the wire is wound around the drum. The rotation of the servomotor (normal or reverse rotation) is controlled by the PLC, and the ascent speed of the camera is maintained constant by the AC servomotor. Limit switches ⑦ are attached to the upper and lower parts of the support pillar as stop points for the camera. Images captured by the camera are transmitted to the PC via an Ethernet cable for image processing.

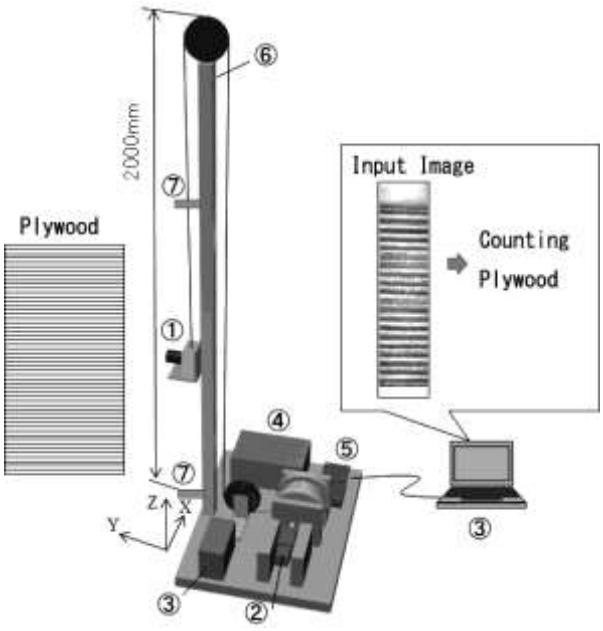

Figure 4-3 Apparatus configuration

4.3.2 Measurement procedure

The procedure for measuring the number of stacked plywood sheets is described step follows, with reference to Figure 4-3.

(1) Normal rotation of the servomotor is first started. As the camera begins to rise, line images are transmitted to the image-processing PC. Image transmission is repeated until the camera arrives at the upper limit switch.

(2) When the camera arrives at the upper limit switch, reverse rotation of the servomotor is started, and the servomotor is turned off until the camera reaches the lower limit switch.

(3) Image processing is implemented using the information recorded by the PC, and the number of plywood sheets is determined.

4.3.3 Measurement of the number of plywood sheets using normalized cross-correlation

When the color gradation of the plywood cross-section has large variations compared to the tangential direction, the brightness of the normal direction is periodical and the amplitude is large. Therefore, the NCC method is suitable for measuring number of the plywood sheets in this situation.

(1) Normalized cross-correlation

The top-left corner of the inspection image is assumed as the origin of the coordinate system. The vertical direction is set as the I axis, and the horizontal direction is set as the J axis. Thus, the I axis coincides with the normal direction of the stacked plywood sheets, and the J axis coincides with the tangential direction. The size of the inspection image is assumed to be m rows by n columns. The coordinate on the I axis is indicated as i, and the coordinate on the J axis is indicated as j, the brightness of each pixel is denoted as $a_{i,j}, (i = 1, \cdots, m, j = 1, \cdots, n)$, and the mean brightness is denoted by $\bar{a}$. A number of template images of stacked plywood cross-sections are prepared. The size of the template image is assumed to be

s rows by n columns. The brightness of each pixel is denoted by $t_{v,j}, (v = 1, \cdots, s, j = 1, \cdots, n)$, and the mean brightness is denoted by $\bar{t}$. In the present study, for the J axis, the inspection image and template image are the same size. An area of the inspection image the same size as the template image is scanned in the direction of the I axis. The normalized cross-correlation $r_i, (i = 1, \cdots, m)$ is calculated as follows:

$$r_i = \frac{\sum_{v,j}(a_{i+v} - \bar{a})(t_{v,j} - \bar{t})}{\sqrt{\sum_{v,j}(a_{i+v} - \bar{a})^2 \cdot \sum_{v,j}(t_{v,j} - \bar{t})^2}} \qquad (4.1)$$

The normalized cross-correlations are obtained from a number of template images, and the normalized cross-correlation (NCC) maxima are taken as the correlation coefficients of the i coordinate in the inspection image. The correlation coefficients indicate a periodically changing waveform in the I axis direction, and the maximum correlation coefficient appears at the boundary between adjacent plywood sheets. As such, the number of NCC maxima satisfying the following conditions is taken as the number of plywood sheets.

(2) Selecting the NCC maxima condition

Stacked plywood sheets have gaps between adjacent sheets because of the tolerances for warpage and torsion of plywood sheets. The brightness values of these gaps are very similar to those of the core veneer. So, when using only Eq. (4.1), there is a possibility that some of the gaps can be erroneously identified as core veneers. However, an interval between two adjacent core veneers is approximately equal to the thickness of a plywood sheet, whereas the interval between a core veneer and the adjacent gap is much smaller than the thickness of a plywood sheet, and the correlation coefficient at the core veneer is also smaller. Figure 4-4 shows a diagram of the results obtained using the NCC method.

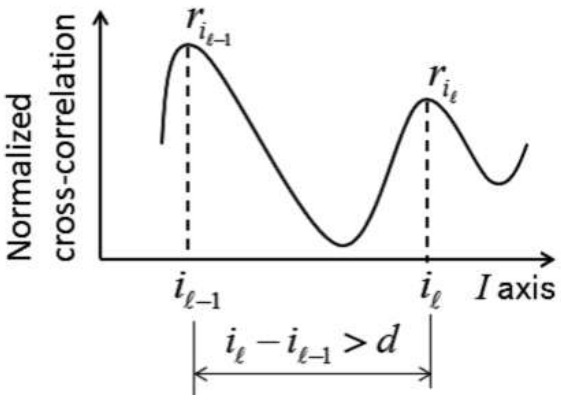

Figure 4-4 Diagram of the results obtained by the NCC method

The number of NCC maxima that satisfies the following equation is used as the number of plywood sheets, and other peaks are excluded:

$$\left((i_\ell - i_{\ell-1}) > d\right) \cap \left(r_{i_\ell} > h\right) \qquad (4.2)$$

Where, symbol $l(l = 1, \cdots, NL)$ represents serial numbers of local peaks of NCC. Symbol i_ℓ represents a coordinate of the $\ell\, th$ local peak of NCC and r_{i_ℓ} represents the value of NCC at the coordinate i_ℓ. Symbol d represents the lower limit of the interval between the coordinate of consecutive NCC maxima. In the present study, an image of a known number of stacked plywood sheets is used as the reference image. Based on a preliminary experiment, the average interval between adjacent NCC maxima μ_1, average NCC maxima μ_2, and the standard deviation of NCC maxima σ_2 are obtained using the following equations.

$$\mu_1 = \frac{1}{NL-1}\sum_{l=2}^{NL}(i_l - \mathrm{i}_{l-1}) \qquad (4.3)$$

$$\mu_2 = \frac{1}{NL}\sum_{l=2}^{NL} r_{i_l} \qquad (4.4)$$

$$\sigma_2 = \frac{1}{NL}\sum_{l=1}^{NL}\left(r_{i_l} - \mu_2\right)^2 \qquad (4.5)$$

The interval between a core veneer and the adjacent gap is considered to be half the average sheet thickness $(d = \mu_1/2)$, and the lower limit of NCC maxima is set as $h = \mu_2 - 3.5\sigma_2$.

4.3.4 Measurement of the number of plywood sheets in a stack using an estimation model

(1) Feature based on the brightness

The method using NCC described in Section 4.3.3 is based on the assumption that there is a significant difference in the color gradation between the core veneer and the face veneer of a sheet. However, if this difference is not so large, the inspection result is not accurate. In seeking to address this shortcoming, we found that the variation of the brightness in the J axis direction of the face veneer is larger than that of the core veneer. Based on previous studies [74], the mean, variance, standard deviation, skewness, and kurtosis of brightness are used as the features, and the sum of absolute differences used in the SAD method (Eqs.（4.6）- (4.12)) is also used. The first line ($i = 1$) of the image input corresponds to a background area. Since the background area is monochrome, no difference is found in the brightness values. Accordingly, the feature value $x_{1,7}$ at the first line ($i = 1$) of the image input in Eq.(4.12) is set as 0. Using these features, an estimation model is selected to accurately identify the core veneer of the sheets, even in the areas where the difference in the brightness of the core veneer and the face veneer is small.

$$x_{i,1} = \frac{1}{n}\sum_{j=1}^{n} a_{ij} \quad (4.6)$$

$$x_{i,2} = \frac{1}{n-1}\sum_{j=1}^{n}\left(a_{ij} - x_{i,1}\right)^2 \quad (4.7)$$

$$x_{i,3} = \sqrt{x_{i,2}} \quad (4.8)$$

$$x_{i,4} = \frac{1}{n}\sum_{j=1}^{n}\left(\frac{a_{ij}-x_{i,1}}{x_{i,3}}\right)^3 \quad （4.9）$$

$$x_{i,5} = \frac{1}{n}\sum_{j=1}^{n}\left(\frac{a_{ij}-x_{i,1}}{x_{i,3}}\right)^4 \quad （4.10）$$

$$x_{i,6} = \sum_{j=1}^{n-1}\left|a_{i,j+1} - a_{ij}\right| \quad (4.11)$$

$$x_{i,7} = \sum_{j=1}^{n}\left|a_{i-1,j} - a_{ij}\right| \quad (4.12)$$

(2) Reference image

A reference image is prepared for setting the control variables of the estimation model, and the seven features are obtained using Eqs.(4.6) – (4.12). The boundary between the core veneer and the face veneer is then visually determined, and the output values are set as 1 for the core veneer and 0 for the face veneer. An estimation model is then selected to express the relationship between the seven feature values and the output values.

(3) Selection of an estimation model based on the cross-validation method

The K-fold cross-validation method is used to find the estimation model with the lowest generalization error among various types of models [75]. The feature value is represented by an N-dimensional input vector, $\vec{x} = (x_1, \cdots, x_N)^T \in R^N$, and the output value is defined as $y \in R$, where the core veneer (output value = 1) and face veneer (output value = 0) are already known. Then, the input/output pair can be denoted by $(\vec{x}_i, y_i)$. If the control variable $\vec{\omega}$ and estimation model variable θ are defined, the estimation model for the input/output pair can be expressed as follows:

$$y = f(\vec{x}, \vec{\omega}, \theta) \qquad (4.13)$$

As mentioned earlier, the decision tree, linear discriminant function, and neural network have been used in previous studies [76-78]. For example, when the estimation model variable θ is the decision tree model, the elements of the control variable $\vec{\omega}$ are the branching conditions (e.g., features such as brightness and threshold) of the nodes in the classification tree. The input/output pairs are represented by a data set, $D = \{(\vec{x}_i, y_i), \cdots (\vec{x}_m, y_m)\}$. The data set, D, is equally divided into K groups, and the uth test set is C_u, $(u = 1, \cdots, K)$. If the test set, C_u, is removed from the data set, D, we can obtain the training set, $L_u(D/C_u)$. The training data set is used to obtain the control variable of the estimation model. The test data set is used for assessment of the generalization error of the final chosen model once the control variable is determined. The generalization error $E(\theta)$ obtained by K-fold cross validation method is expressed by Eq. (4.14)

$$E(\theta) = \frac{1}{2}\sum_{u=1}^{K}\sum_{(\vec{x},y)\in C_u}\left(y - f(\vec{x}, \vec{\omega}_u^*, \theta)\right)^2 \qquad (4.14)$$

The data set is divided into a training set and a test set for the calculation of $E(\theta)$. Using $f(\vec{x}, \vec{\omega}_u^*, \theta)$, which uses the best fitting control variable, $\vec{\omega}_u^*$, for training set L_u, the performance of the estimation model can be asymptotically evaluated if we can accurately determine whether the test data are properly associated with the learning data. Then, the model with the smallest generalization error $E(\theta)$ is selected as the estimation model. The estimation model is determined using the above procedures. Once the estimation model is decided, a newly input image is tested to identify the core veneer and face veneer for each line in the I axis direction.

(4) Correction of estimation results

Both core veneer and face veneer can be erroneously detected because of uneven brightness. False detection situations can be classified into four types, as shown in Figure 4-5.

Figure 4-5 (a) shows an example of an extremely narrow interval with an output value of 1 (false detection 1). False detection occurs because of warping of the plywood sheets, for example. The brightness of the gap is low enough to generate an output value of 1, and the gap is falsely detected as core veneer. However, the thickness of the actual gap is approximately 0.1 mm, while the thickness of the core veneer is greater than 1 mm, which is a significant difference.

Figure 4-5 (b) shows an example of an extremely narrow interval with an output value of 0 (false detection 2). Although the mean brightness of the core veneer is lower than that of the face veneer, there are areas in which the brightness of the core veneer is similar to that of the face veneer. Therefore, the variance of the brightness of the core veneer, $x_{i,2}$, is not 0. Then, the output value may be determined to be 0 by the estimation model for a very small region having high brightness that appears on the J axis.

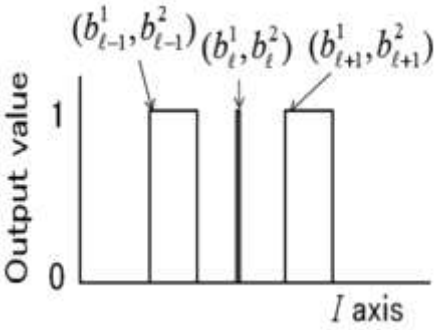

(a） False detection 1 (extremely narrow interval with an output value of 1)

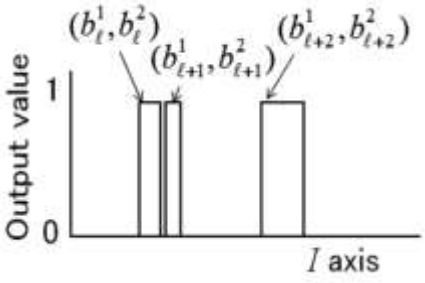

(b)False detection 2 (extremely narrow interval with an output value of 0)

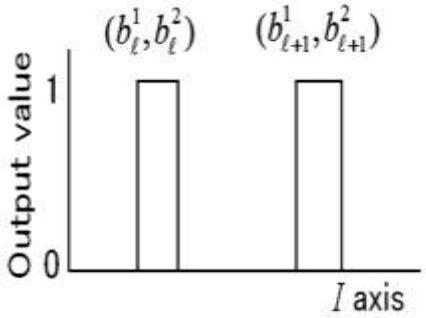

(c)False detection 3 (extremely wide interval with an output value of 0)

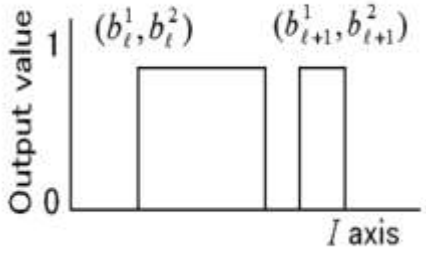

(d)False detection 4 (extremely wide interval with an output value of 1)

Figure 4-5　False detection situations

Figure 4-5 (c) shows an example of an extremely wide interval with an output value of 0 (false detection 3), and Figure 4-5 (d) shows an example of an extremely wide interval with an output value of 1 (false detection 4). When the brightness of the stacked plywood cross-section is very different from the brightness of the reference image used in the estimation model, false detection 3 or 4 may occur. The following procedure is proposed in order to prevent the four types of false detections shown in Figure 4-5.

4.4　Application Example

4.4.1　Experimental conditions

Table 4-1 Experimental conditions

Number of plywood sheets	500
Sheet thickness (specification)	2.4 mm
Height of stacked plywood (measured value)	1,264.5 mm
Average thickness (measured value)	2.45 mm
Camera ascent speed	18.3 mm/s
Image input speed	558 lines/s

We used the apparatus shown in Figure 4-3 to conduct the experiments to measure the number of plywood sheets in a stack. The measurement object was 500 common plywood sheets, and the standard thickness of each sheet was 2.4 mm. A total of 50 plywood sheets were selected randomly from the 500 sheets, and the thickness of the stack of 50 plywood sheets was measured using a micrometer. The average sheet thickness was calculated to be 2.45 mm, and the standard deviation was 0.04 mm. The height of the 500 stacked plywood sheets was measured at each of the four corners of the stack, and at the measurement position of the line sensor camera, which was adapted to move vertically. Measurements were repeated for five different stacking sequences of the sheets to obtain the average height of the stack. The mean height was 1,264.5 mm and the standard deviation was 0.6 mm, which indicates that there were multiple gaps between the sheets. Moreover, dividing the height of the stack (1,264.5 mm) by the average sheet thickness (2.45 mm) indicates that the number of sheets should be 516. This confirms the difficulty of estimating the number of plywood sheets in a stack on the basis of the height of the stack. The experimental conditions, including the camera ascent speed and image input speed, are listed in Table 4-1. Additionally, the difference in mean brightness between the core veneer and face veneer was around 100.

4.4.2 Measurement of the number of plywood sheets using normalized cross-correlation

(1) Preliminary experiment

In order to prevent false detection caused by gaps, a preliminary experiment was performed using 50 stacked plywood sheets as the measurement object. Three images were chosen as template images, which were obtained separately from the upper, middle and lower parts of the stack of plywood sheets. The sheet thickness (pixels) was obtained from the average sheet thickness, the camera ascent speed and the image input speed, which was calculated to be 37 (= 2.45/18.3 × 558/2) pixels for the constant d. Figure 4-6 shows the correlation coefficient obtained using Eq. (4.1), where the horizontal axis represents the i coordinate of the inspection image and the vertical axis represents the correlation coefficient of the template image. The number of NCC maxima was the same as the number of plywood sheets. Average NCC maximum μ_2 was 0.77 and standard deviation σ_2 was 0.06. At the positions of the three template images, the correlation coefficient was confirmed to be 1.0. As shown in Figure 4-6, the average interval between the adjacent maxima μ_1 was 85.1 pixels and the standard deviation $\sigma_1$was 5.8 pixels. Based on this information, we obtained the following constants for the experiment: $d = 42.5\ (= 85.1/2)$ and $h = 0.55\ (= 0.77 - 3.5 \times 0.06)$. The average interval between adjacent maxima μ_1 was greater than 37 pixels, which was an indirect indication of the existence of gaps between plywood sheets.

(2) Measurement results for the number of plywood sheets

For the inspection image of 500 stacked plywood sheets, as a result of calculating the correlation coefficients using the NCC method, 500 NCC maxima were detected. Figure 4-7 shows the intervals between adjacent NCC maxima. The mean interval was 86.1 pixels and the standard deviation was 5.2 pixels. The mean value was

greater than that obtained in the preliminary experiment. The horizontal lines indicate three standard deviations above and below the mean. All of the intervals were higher

than the minimum critical value (42.5 pixels). The calculation time required for template matching was 43.2 s. Although the time required to obtain the inspection image was not included in the total time, the measurement time was significantly shortened compared to the current working time of 240 s.

The experiments were performed 20 times using a different number of plywood sheets, ranging between 450 and 500. The results of the 20 experiments are shown in Table 4-2. The mean calculation time was 36.0 s. For the situation in which the difference in mean brightness between the core veneer and face veneer was around 100, the total number of plywood sheets could be correctly determined using the NCC method.

Table 4-2 Results of the preliminary experiment

[ ]: Number of cases

	NCC	Estimation model
Accuracy rate	1.0	1.0
Estimated error	0[20]	0[20]
Calculation time(s)	36	6.2

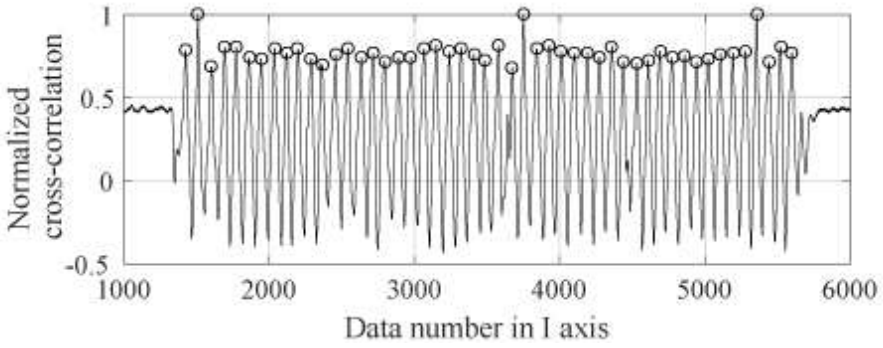

Figure 4-6 Normalized cross-correlation obtained in the preliminary experiment

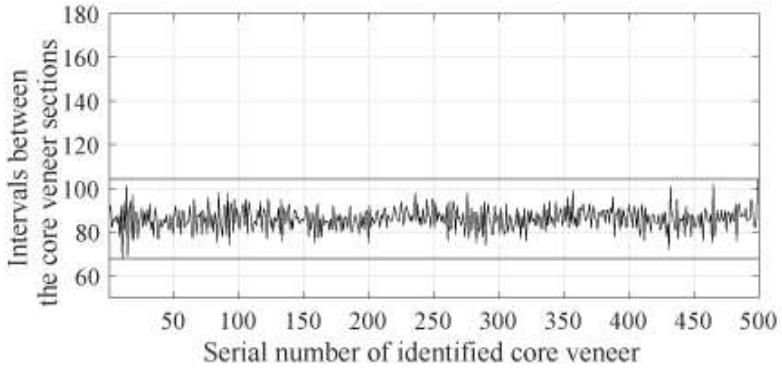

Figure 4-7 Intervals between core veneer sections

4.4.3 Measurement of the number of plywood sheets using the estimation model

(1) Preliminary experiment

An image of 50 stacked plywood sheets was used as the reference image in the preliminary experiment. The reference image was visually confirmed to identify the boundary between the core veneer and face veneer sections. The output value was set to 1 for core veneer and 0 for face veneer. The feature values of the core veneer and face veneer sections were obtained using Eqs 4.6 through 4.12. As a result, 4,279 data sets were obtained, including 2,487 core veneer data sets, and 1,792 face veneer data sets.

The critical values $(D_1, D_2, D_3, \text{and } D_4)$, which were used for correcting the estimation results, were then selected. The average thickness of the core veneer section was visually confirmed to be 48.0 pixels and the standard deviation was 6.6 pixels. The mean interval between adjacent core veneer sections was confirmed to be 85.1 pixels, with a standard deviation of 6.7 pixels. The critical value, D_1, for the judgment of false detection 1 was $24.5(= 48.0 - 3.5 \times 6.7)$. We obtained critical values $D_2 = 61.6(= 85.1 - 3.5 \times 6.7)$, $D_3 = 108.5(= 85.1 + 3.5 \times 6.7)$, and $D_4 = 71.1(= 48.0 + 3.5 \times 6.7)$ for the judgment of false detections 2,3, and 4 respectively in a similar manner.

Using the data sets obtained from the reference image, the estimation performance

of the decision tree, linear discriminant function, and neural network models could be compared. The Gini coefficient was used for node branching in the decision tree model. The neural network model had three layers: an input layer, a middle layer and an output layer. The input layer contained seven nodes and the middle layer contained 15 nodes. The transfer function used in the middle layer was a sigmoid function, whereas the transfer function sued in the output layer was a linear function.

The generalization errors obtained from the K-fold cross-validation method for each estimation model is shown in Table 4-3. If the division number, K, was set to 10, the generalization error of the decision tree model was the smallest. In the decision tree model, 14 control variables (a classification tree with 14 nodes) were chosen for classification. In the neural network model, the number of control variables was significantly larger compared to the decision tree model and linear discriminant function model.

(2) Measurement of the number of plywood sheets using the estimation model

Using the decision tree model selected in the previous section, the position of the core veneer sections were estimated using an inspection image of 500 stacked plywood sheets. The partial estimation results are shown in Figure 4-8. A total of 500 positions were estimated as positions of core veneer sections. Figure 4-8(a) shows the lower part of the stack with the I coordinate values increasing downward from 200 to 1,000. Correspondingly, in real space, the camera is ascending from the bottom to the top of the stack in the Z axis direction. The range in which the i coordinate varied from 1 to 370 is the background. The graph on the right-hand-side of Figure 4-8(a) shows the output value of the inspection image in the I axis direction. The output value is 0 at a position on the face veneer and 1 at a position on the core veneer. A comparison of the inspection image on the left and the output value image on the right indicates that the positions of the eight plywood core veneer sections were correctly detected. Figure 4-8 (b) shows the detection results for core veneer sections at the middle part of the stack (the 200th to 209th sheets). The core veneer sections were

detected at equal intervals. Figure 4-8(c) shows the detection results for core veneer sections at the upper part of the stack (the 493th to 500th sheets).

Then the interval between adjacent core veneer sections was examined.

Figure 4-9 shows the results obtained for all of the intervals between adjacent core veneer sections, where the interval was defined as the interval from the lth core veneer to the $(l+1)$th core veneer$(l = 1, \cdots, 499)$. The mean interval was calculated to be 86.1 pixels and the standard deviation was 7.8 pixels. The horizontal lines indicate three standard deviations above and below the mean. All intervals were less than 110 pixels throughout the entire sample, which indicated that all of the core veneer sections were detected. Compared with the NCC method used in the previous section, there was no remarkable difference in the average interval between adjacent core veneer sections.

The experiment was performed another 20 times using different numbers of plywood sheets, ranging between 450 and 500. The results of the experiment are shown in Table 4-2, and the number of plywood sheets was measured correctly in each instance. The accuracy rate of this method was also 1.0 compared to the NCC method. Moreover, the calculation time required for the estimation model method was 6.2s, which is much quicker than that for the NCC method (36.0 s). The above results indicate that the estimation model method is more suitable for practical use than the method using normalized cross-correlation.

Table 4-3 Generalization errors of the estimation models

Estimation models	Generalization errors
Decision tree model	9.5
Linear discriminant function model	50.0
Neural network model	145.0

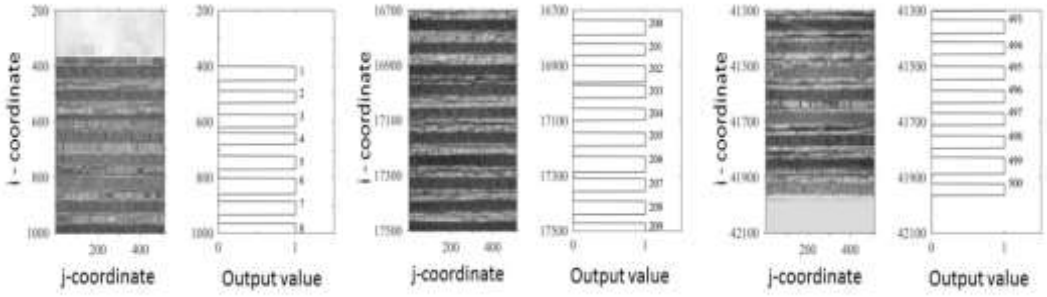

(a) Lower part of the stack (I axis: 200-1,000)

(b) Central part of the stack (I axis: 16,700-17,500)

(c) Upper part of the stack (I axis: 41,300-42,100)

Figure 4-8 Measurement results obtained using the decision tree model

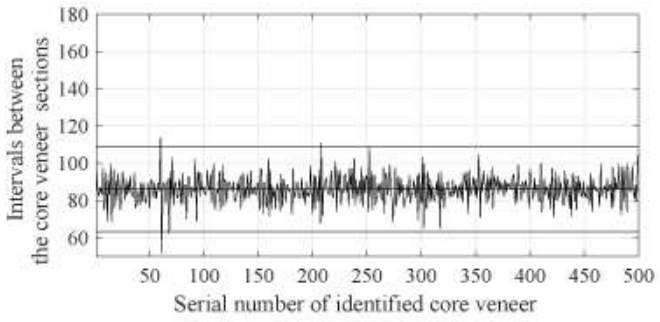

Figure 4-9 Intervals between core veneers estimated by the decision tree

4.4.4 Comparison of comparative method and proposed method

As described in Section 4.4.2 and Section 4.4.3, both of the comparative method and proposed method can accurately measure the number of 450-500 stacked plywood sheets. Besides, we also investigated the measurement time required to perform the inspection task.

The inspection task was performed by seven workers: four unskilled workers without experience and three skilled workers. The unskilled workers required approximately 285 s to inspect (count) 500 stacked plywood sheets whereas the skilled workers required approximately 210s. The average time from inputting the image to obtaining the measurement result was approximately 120s. The method

using the estimation model reduced the inspection time by 58% for unskilled workers and 43% for skilled workers. Furthermore, the inspection image and the measurement results can be saved as inspection data, which enables inspection information to be passed on to the shipping destination.

4.5 Conclusion

In the present paper, we proposed two methods and an apparatus for automating the task of counting stacked plywood sheets. The results of this study are summarized as follows.

Two methods for measuring the number of plywood sheets in a tack using an inspection image were proposed. The comparative method is based on the NCC method. The inspection image is scanned in the I axis direction and the cross-correlations of the template image of the cross-section of the plywood stack is then used to obtain the number of normalized cross-correlation maxima, which is equal to the number of plywood sheets. The proposed method is based on the cross-validation method, which uses an estimation model to identify core veneer sections and face veneer sections in the cross-section of the plywood stack. The plywood sheets are measured one-by-one from the inspection image using the estimation model.

The accuracies of the two methods were compared through an application example. When the difference in brightness between the core veneer and face veneer sections was 100 or more, no measurement error occurred for either method. However, the visual measurement time was reduced by more than 40% using the proposed method involving the estimation model.

Chapter 5 Conclusions

In this thesis, an important issue of improving sensor technology application is addressed in warehousing from the perspective of optimization based on unknown data. Sensor systems including an indoor positioning system, a work analysis automation system and a visual inspection system are established and their performances are evaluated through application examples. The topic is motivated by the new practical and theoretical challenges as emerged from the "sensor decade" with respect to information and communication technology development.

Firstly, the background of distribution process in warehousing is analyzed to propose the crucial concentration about improving generalization ability of estimation models used in three sensor systems for reducing warehouse management cost. After that, purpose, significance and organization of the study are proposed by analyzing the related literatures and their applications about sensor systems used in warehousing.

Secondly, an indoor positioning system using RFID is designed in order to resolve the existed problem of multipath caused by radio interference. The system is used to both estimate the location and height of a stationary object, and the flow line of a moving object. Then, the system is evaluated through application example, and the evaluation result for the stationary object is good enough for practical use, however, the estimation of flow line is not so accurate for site monitoring. Besides, the system designed improves the estimation performance by using multi tags at different height for estimation, which could help to reduce the interference caused by multi radio wave paths.

Thirdly, the work automation system including the unresolved problem about flow line measurement and a new proposal about motion analysis are studied. An ultrasonic system is mainly used to analyze the whole process of a picking work in order to improve the work efficiency in distribution processing. Through an

application example at a retail clothing distribution center, the accuracy of the system is evaluated by comparing the estimated result with the video records. The result revealed the reliability of the system for practical use. While using this system, the method of using three or two receivers to estimate the transmitter's position is proposed for better estimation performance, which was newly proposed by the present study.

Lastly, a visual inspection system is designed for automating the task of counting stacked plywood sheets. A traditional method based on NCC method was selected as a comparative method and an estimation method based on cross-correlation as proposed method, and the accuracies of the two methods were compared through an application example, no measurement error occurred for both methods when the sheet number is more than 100. But according to the application example, the estimation method based on cross-correlation method can reduce the time needed for counting by more than 40%, which is thought to be more appropriate for the checking task.

With the strong focus on practical relevancy, the sensor systems and the mathematical methods developed in this thesis could be used widely in practical work at warehouses and distribution centers. Indoor positioning system was developed to resolve warehouse management problem of finding items and idle space, and also the system is able to estimate height of the tags exactly, and this can be used to judge which layer of the shelf the required items are placed on. And so combining the location and height estimation information, it is possible to find exactly where the required items are in a short time. Besides, since place information of all the inventories can be obtained using this system, it is easy to find the idle space which has been not used sufficiently, and this is the basic information for storage space optimization. Work analysis automation system was developed to help picking out items more efficiently and avoid losing items. Using the proposed system, it is possible to get a worker's flow line during the whole inbound or outbound work process, which can be analyzed to improve the whole picking out process. Besides, combining with indoor positioning method proposed in Chapter 2, it is possible to

record and analyze the whole working process and then to figure out when and where a certain item was picked out, which can be used for tracking items to reduce the probability of losing items. The method proposed in Chapter 4 is developed for a certain task of counting stacked plywood sheets. However, the proposed estimation model method used in a sensor system can also be applied to other outbound inspection work such as counting items and quality control.

Moreover, using the machine learning algorithms with the improving conception, we hope that much more sensor systems used in warehousing could be evaluated and improved at intervals according to different environment and conditions to improve the work efficiency of the distribution process.

References

[1] Barreto, L., Amaral, A. and Pereira, T., Industry 4.0 Implications in Logistics: An Overview, Procedia Manufacturing, Vol. 13, (2017), pp. 1245-1252.

[2] Speranza, M. G., Trends in Transportation and Logistics, European Journal of Operational Research, Vol. 264, Issue 3, (2017), pp. 830-836.

[3] Ackerman, K. B., Practical Handbook of Warehousing, Springer Science & Business Media, (2012), p. 10.

[4] Sarac, A., Absi, N. and Dauzère-Pérès, S., A Literature Review on the Impact of RFID Technologies on Supply Chain Management. International Journal of Production Economics, Vol. 128, Issue 1, (2010), pp. 77-95.

[5] Connolly, C., Warehouse Management Technologies, Sensor Review, Vol. 28, No. 2, (2008), pp. 108-114.

[6] Yan, B., Chen, Y. and Meng, X., RFID Technology Applied in Warehouse Management System, 2009 ISECS International Colloquium on Computing, Communication, Control, and Management , IEEE Computer Society, Vol. 3, (2008), pp. 363-367.

[7] Ross, D.F., Distribution Planning and Control, Springer, (2015), p. 606.

[8] Poon, T. C., Choy, K. L., Chan, F. T., Ho, G. T., Gunasekaran, A., Lau, H. C. and Chow, H. K., A Real-time Warehouse Operations Planning System for Small Batch Replenishment Problems in Production Environment, Expert Systems with Applications, Vol. 38，Issue 7, (2011), pp. 8524-8537.

[9] Horvath, L., Collaboration: The Key to Value Creation in Supply Chain Management, Supply Chain Management, Vol. 6, Issue 5, (2001), pp. 205-207.

[10] Ackerman, K. B., Practical Handbook of Warehousing, Springer Science & Business Media, (2012), p. 10.

[11] Wilson, J. S., Sensor Technology Handbook, Newnes, (2005), p. 18.

[12] Akyildiz, I. F., Su, W., Sankarasubramaniam, Y. and Cayirci, E., A Survey on Sensor Networks, IEEE Communications Magazine, Vol. 40, Issue 8, (2002), pp. 102-114.

[13] Wilson, J. S., Sensor Technology Handbook, Newnes, (2005), p. 576.

[14] García-Hernando, A. B., Martínez-Ortega, J. F., López-Navarro, J. M., Prayati, A. and Redondo-López, L., Problem Solving for Wireless Sensor Networks, Springer Science & Business Media, (2008), pp. 177-179.

[15] Zhou, J. and Shi, J., RFID Localization Algorithms and Applications—A Review, Journal of Intelligent Manufacturing, Vol. 20, Issue 6, (2009), p. 695.

[16] Ijaz, F., Yang, H. K., Ahmad, A. W. and Lee, C., Indoor Positioning: A Review of Indoor Ultrasonic Positioning Systems, 15th International Conference on Advanced Communications Technology (ICACT), (2013), pp. 1146-1150.

[17] Mainetti, L., Patrono, L. and Sergi, I., A Survey on Indoor Positioning Systems, 22nd International Conference on Software, Telecommunications and Computer Networks (SoftCOM) , (2014), pp. 111-120.

[18] Ullrich, G., Automated Guided Vehicle Systems, Springer, (2015), pp. 1-14.

[19] Nof, S.Y., Ceroni, J., Jeong, W. and Moghaddam M., Revolutionizing Collaboration through e-Work, e-Business, and e-Service, Automation, Collaboration, & E-Services, Springer, Vol. 2, (2015), pp. 273-313.

[20] Ji, S. and Niu, X., Application of DAS in Cold Chain Logistics Warehousing System Based on WMS, Proceedings of the International Conference on Green Communications and Networks, Vol. 113, (2012), pp. 1603-1610.

[21] Alpaydin, E., Introduction to Machine Learning, MIT press, (2014), p. 1.

[22] Duffy A. H., The “What” and “How” of Learning in Design, IEEE Expert, Vol. 12, Issue 3, (1997), pp. 71–76.

[23] Alsheikh, M. A., Lin, S., Niyato, D. and Tan, H. P., Machine Learning in Wireless Sensor Networks: Algorithms, Strategies, and Applications, IEEE Communications Surveys & Tutorials, Vol. 16, No. 4, (2014), pp. 1996-2018.

[24] Richards, G., Warehouse Management: A Complete Guide to Improving Efficiency and Minimizing Costs in the Modern Warehouse, Kogan Page Publishers, (2017), pp. 5-6.

[25] Kilinc, O., Kucukyildiz, G., Karakaya, S. and Ocak, H., Image Processing Based Indoor Localization System, Signal Processing & Communications Applications Conference, (2014), pp. 1654-1657.

[26] Ko, C. H., RFID 3D Location Sensing Algorithms, Automation in Construction, Vol. 19,

Issue 5, (2010), pp. 588-595.

[27] Ijaz, F., Yang, H. K., Ahmad, A. W. and Lee, C., Indoor Positioning: A Review of Indoor Ultrasonic Positioning Systems, 2013 15th International Conference on Advanced Communications Technology (ICACT), (2013), pp. 1146-1150.

[28] Szeliski, R., Computer Vision: Algorithms and Applications, Kyoritsu Shuppan, (2013), pp. 279- 353. (in Japanese)

[29] Minami, M.， Morikawa, H. and Aoyama, Y., Design and Implementation of Autonomous Decentralized Position Detection System Using Ultrasonic Wave, The Journal of Institute of Electronic, Information and Communication Engineerings, Vol. 88, Issue 12, (2005), pp. 1432-1441.

[30] Ozsoy, K., Bozkurt, A. and Tekin, I., Indoor Positioning Based on Global Positioning System Signals, Microwave & Optical Technology Letters, Vol. 55, Issue 5, (2013), pp. 1091-1097.

[31] Murata, M., Segawa, J. and Torimoto, H., Development of IMES Technology: New Techniques of Seamless Three-Dimensional Positioning and Navigation, The Journal of Institute of Electronic, Information and Communication Engineerings, Vol. 95, Issue 2, (2012), pp. 119-124.

[32] Matsumura, S., Kanamori, C., Shijo, R. and Matsumoto, K., Development of the Sensor Fusion System for Seamless Indoor/Outdoor Navigation, Spring Meeting of the Japan society for precision engineering, (2016), pp. 879-880. (in Japanese)

[33] Kitasuka,T., Nakanishi, T. and Fukuda, A., Indoor Location Sensing Technique Using Wireless Network, Journal of Information Processing, Vol. 44, Issue 10, (2003), pp. 131-139.

[34] Tsuji, H., Experimental Verification of Location Estimation Indoor and Outdoor Using Array Antenna, The Journal of Institute of Electronic, Information and Communication Engineerings, Vol. 90, Issue B(9), (2007), pp. 784-796.

[35] Alarifi, A., Alsalman, A. M., Alsaleh, M., Alnafessah, A., Alhadhrami, S., Mai, A. A., et al., Ultra Wideband Indoor Positioning Technologies: Analysis and Recent Advances. Sensors, Vol. 16, Issue 5, (2016), pp. 1-36.

[36] Luh, Y.P. and Liu, Y.C., Reading Rate Improvement for UHF RFID Systems with Massive Tags by the Q Parameter. Wireless Personal Communications, Vol. 59, Issue 1, (2011), pp. 147-157.

[37] Sadr, R., Stephens, S. and Jones, C., Radio frequency identification tag location estimation and tracking system and method: U.S. Patent No. 8,072,311, U.S. Patent and Trademark Office, (2011).

[38] Sekiguchi, T.， Yu, Y., Kajihara,Y.， Mukai, T., Hirata, K., Hida, T. and Eguchi, M., Development of RFID Positioning System Using Neural Network Model, Asia-pacific Journal of Industrial Management, Vol. 5, Issue 1, (2014), pp. 8-16.

[39] He, X., Ye, D., Peng, L., Ruchuan, W. and Yizhu, L., An RFID Indoor Positioning Algorithm Based on Bayesian Probability and K-nearest Neighbor, Sensors, Vol. 17, Issue 8, (2017), p. 1806.

[40] Ming, K. L., Bahr, W. and Leung, S. C. H., RFID in the Warehouse: A Literature Analysis (1995–2010) of Its Applications, Benefits, Challenges and Future Trends, International Journal of Production Economics, Vol. 145, Issue 1, (2013), pp. 409-430.

[41] Izumi, K., Sato, Y., Kajihara, Y. and Taki, S., Productivity Improvement in Distributive Processing for Fashion Goods Based on Work Analysis, Journal of Japan Industrial Management Association, Vol. 64, No. 2, (2013), pp. 169-176. (in Japanese)

[42] Lu, W., McFarlane, D., Giannikas, V. and Zhang, Q., An Algorithm for Dynamic Order-picking in Warehouse Operations, European Journal of Operational Research, Vol. 248, Issue 1, (2016), pp. 107-122.

[43] Enkawa, T., Dumrongkit, R. and Akiba, M., A Consideration on Methods to Measure Efficiency of Order-Picking by Introduction of IQ-Curve, Journal of Japan Industrial Management Association, Vol. 35, No. 1, (1984), pp. 50-56.

[44] Matusiak, M., de Koster, R. and Saarinen, J., Utilizing Individual Picker Skills to Improve Order Batching in a Warehouse, European Journal of Operational Research, Vol. 263, Issue 3, (2017), pp. 888-899.

[45] Sakuma, A., Trend of New Techniques in Work Study, Journal of Japan Industrial Management and Association, Vol. 28, No. 1, (1977), pp. 20-26. (in Japanese)

[46] Zhang, M., Liang, S., Kajihara, Y. and Fukunaga, K., Development of Method and Apparatus for the Work Analysis in Warehouse Operation, Proceedings of ICIM 2016, (2016), pp. 516-522.

[47] Manghisi, V. M., Uva, A. E., Fiorentino, M., Bevilacqua, V., Trotta, G. F. and Monno, G.,

Real Time RULA Assessment Using Kinect V2 Sensor, Applied Ergonomics, Vol. 65, (2017), pp. 481-491.

[48] Bortolini, M., Faccio, M., Gamberi, M. and Pilati, F., Motion Analysis System (MAS) for Production and Ergonomics Assessment in the Manufacturing Processes, Computer & Industrical Engineering, (2018), (in press) https://doi.org/10.1016/j.cie.2018.10.046.

[49] Seemanthini, K. and Manjunath, S., Human Detection and Tracking using HOG for Action Recognition, Procedia Computer Science, Vol. 132, (2018), pp. 1317-1326.

[50] Enohara, T., Baba, K. and Ohmura, A., Measuring Pedestrian Trajectories Utilizing Stereo Vision, ITS Workshop 2007 of Information Processing Society of Japan, Vol. 2007, Issue 90, (2007), pp. 83-86. (in Japanese)

[51] Choe, N., Zhao, H., Qiu, S. and So, Y., A Sensor-to-segment Calibration Method for Motion Capture System based on Low Cost MIMU, Measurement, Vol. 131, (2019), pp. 490-500.

[52] Shuyu, L., Fumoto, A., Kajihara, Y., Tabuchi, Y. and Shinzato, T., Indoor UHF RFID Tag Location Estimation Method, Journal of the Society of Plant Engineers Japan, Vol.30, Issue 1, (2018), pp. 9-18. (in Japanese)

[53] Enohara, T., Baba, K. and Ohmura, A., Measuring Pedestrian Trajectories Utilizing Stereo Vision, ITS Workshop 2007 of Information Processing Society of Japan, Vol. 2007, Issue 90, (2007), pp. 83-86. (in Japanese)

[54] Matsuoka, S., Fujieda, N., Ichikawa, S. and Kawaguchi, H., Development of Real-time Positioning System by Ultrasonic Waves, Journal of the Japan Society of Applied Electromagnetics, Vol. 23, Issue 2, (2015), pp. 380-385.

[55] Shimotsu, M., Kotaki, M., Ogasawara, Y., Yoshimura, N. and Okuyama, D., Detection of Starved Joints in Plywood by Acoustic Emissions, Japanese Journal of Applied Physics, Vol. 27, Issue 1, (1988), p. 64.

[56] Castellani, M. and Rowlands, H., Evolutionary Artificial Neural Network Design and Training for Wood Veneer Classification, Engineering Applications of Artificial Intelligence, Vol. 22, Issue 4-5, (2009), pp. 732-741.

[57] Ito, Y. and Nakano, K., Component Labeling fork: Concave Binary Images Using an FPGA, 2008 IEEE International Symposium on Parallel and Distributed Processing, Vol. 107, No. 390, (2008), pp. 1-8.

[58] Suzuki, H., Hough Transform and Applications, Japan Journal of Industrial and Applied Mathematics, Vol. 9, Issue 3, (1999), pp. 207-219.

[59] Donis-González, I. R. and Guyer, D. E., Classification of Processing Asparagus Sections Using Color Images, Computers and Electronics in Agriculture, Vol. 127, (2016), pp. 236-241.

[60] Shibahara, T., Aoki, T., Nakajima, H. and Kobayashi, K., A High-accuracy Sub-pixel Correspondence Technique Using 1D Phase-only Correlation, IEICE Electronics Express, Vol. 5, Issue 4, (2008), pp. 2343-2356.

[61] Namikawa, M. and Hamada, N., Fast Word Spotting Algorithm for Historical Japanese Document Images, IEICE Technical Report, Vol. 110, No. 467, (2011), pp. 31-36. (in Japanese)

[62] Szeliski R., Computer Vision: Algorithms and Applications, Kyoritsu Shuppan, (2013), pp. 279- 353. (in Japanese)

[63] Saitoh, T., Imamura, M. and Fukui, Y., Development of Initial Inspection System for Wooden Chopsticks by Image Processing, IEICE Transactions on Information and System, Vol. 96, Issue 10, (2013), pp. 2570-2579. (in Japanese)

[64] Sakuma, H., Furukawa, Y., Okada, T., Tanabe, K. and Ueno, S., Image Processing for Visual Inspection of Connector-plug-pins Using Neural Networks, Journal of the Japan Society for Precision Engineering, Vol. 59, Issue 8, (1993), pp. 1325-1330.(in Japanese)

[65] Baba, K. and Hirai, Y., Recognition System of Road Traffic Signs by a Color Video Camera, IEICE Technical Report, Vol. 104, No. 646, (2005), pp. 45-50.

[66] Jiang, P. and Chen, J., Displacement Prediction of Landslide based on Generalized Regression Neural Networks with K-fold Cross-validation, Neurocomputing, Vol. 198, (2016), pp. 40-47.

[67] JFE Steel Coporation, Methods and Apparatus for Counting Stacked Steel Sheets, Japanese Unexamined Patent Application Publication, No. 2016-2:34571 (P2006-23471A). (in Japanese)

[68] Jiang, P. and Chen, J., Displacement Prediction of Landslide based on Generalized Regression Neural Networks with K-fold Cross-validation, Neurocomputing, Vol. 198, (2016), pp. 40-47.

[69] Shuyu, L., Fumoto, A., Kajihara, Y., Tabuchi, Y. and Shinzato, T., Indoor UHF RFID Tag Location Estimation Method, Journal of the Society of Plant Engineers Japan, Vol. 30, Issue 1, (2018), pp. 9-18. (in Japanese)

[70] Choe, N., Zhao, H., Qiu, S. and So, Y., A Sensor-to-segment Calibration Method for Motion Capture System based on Low Cost MIMU, Measurement, Vol. 131, (2019), pp. 490-500.

[71] Cohen, J.A., A Coefficient of Agreement for Nominal Scales, Psychological Bulletin, Vol. 20, Issue 1, (1960), pp. 37-46.

[72] Franzen, M., Kappa Coefficient, Encyclopedia of Clinical Neuripsychology, (2012), p.1389

[73] Landis, J.R. and Koch, G.G., The Measurement of Observer Agreement for Categorical Data, Biometrics, Vol. 33, Issue 1, (1977), pp. 159-174.

[74] Donis-González, I. R. and Guyer, D. E., Classification of Processing Asparagus Sections Using Color Images, Computers and Electronics in Agriculture, Vol. 127, (2016), pp. 236-241.

[75] Jiang, P. and Chen, J., Displacement Prediction of Landslide Based on Generalized Regression Neural Networks with K-fold Cross-validation, Neurocomputing, Vol. 198, (2016), pp. 40-47.

[76] Saitoh, T., Imamura, M. and Fukui, Y., Development of Initial Inspection System for Wooden Chopsticks by Image Processing, IEICE Transactions on Information and System, Vol. 96, No. 10, (2013), pp. 2570-2579. (in Japanese)

[77] Sakuma, H., Furukawa, Y., Okada, T., Tanabe, K. and Ueno, S., Image Processing for Visual Inspection of Connector-plug-pins Using Neural Networks, Journal of the Japan Society for Precision Engineering, Vol. 59, No. 8, (1993), pp. 1325-1330. (in Japanese)

[78] Baba, K. and Hirai, Y., Recognition System of Road Traffic Signs by a Color Video Camera, IEICE Technical Report, Vol. 104, No. 646, (2005), pp. 45-50.